6-2012

Ectopic expression of Rubisco subunits in maize mesophyll cells does not overcome barriers to cell type-specific accumulation

Katia Wostrikoff
Université Pierre et Marie Curie, Paris, katia.wostrikoff@ibpc.fr

Aimee Clark
Boyce Thompson Institute for Plant Research, Ithaca, NY, aimee.l.clark@gmail.com

Shirley Sato
University of Nebraska - Lincoln, ssato1@unl.edu

Thomas E. Clemente
University of Nebraska - Lincoln, tclemente1@unl.edu

David Stern
Boyce Thompson Institute for Plant Research, Ithaca, NY, ds28@cornell.edu

Plant Physiology Preview. Published on June 28, 2012, as DOI:10.1104/pp.112.195677

Running head: Ectopic Rubisco expression in maize

Correspondence to Katia Wostrikoff, Katia.Wostrikoff@ibpc.fr

Journal research area: Systems Biology, Molecular Biology, and Gene Regulation

Ectopic expression of Rubisco subunits in maize mesophyll cells does not overcome barriers to cell type-specific accumulation

Katia Wostrikoff[1,2], Aimee Clark[1], Shirley Sato[3], Tom Clemente[3] and David Stern[1]

1- Boyce Thompson Institute for Plant Research, Tower Rd., Ithaca, NY, USA

2-Centre National de la Recherche Scientifique/Université Pierre et Marie Curie, UMR 7141, Institut de Biologie Physico-Chimique, 13 Rue Pierre et Marie Curie, 75005 Paris, France

3-Department of Agronomy & Horticulture, Center for Biotechnology, Center for Plant Science Innovation, University of Nebraska-Lincoln, Lincoln, NE, USA

FOOTNOTES:

Financial source: This project was supported by the National Research Initiative Competitive Grant no. 2009-35318-05012 from the USDA National Institute of Food and Agriculture to D.S. and K.W., the Nebraska Research Initiative and Center for Plant Science Innovation to T.C. Exchanges between France and USA were funded by the French CNRS-PICS award 5462 to K.W.

Present address: Aimee Clark, 194 Underhill Avenue Apt 3, Brooklyn, NY 11238

Corresponding author: Katia Wostrikoff, Katia.Wostrikoff@ibpc.fr

ABSTRACT

In *Zea mays*, ribulose bisphosphate carboxylase (Rubisco) accumulates in bundle sheath but not mesophyll chloroplasts, but the mechanisms that underlie cell-type specific expression are poorly understood. To explore the coordinated expression of the chloroplast *rbcL* gene, which encodes the Rubisco large subunit (LS), and the two nuclear *RBCS* genes which encode the small subunit (SS), RNAi was used to reduce *RBCS* expression. This resulted in Rubisco deficiency, and was correlated with translational repression of *rbcL*. Thus, as in C3 plants, LS synthesis depends on the presence of its assembly partner SS. To test the hypothesis that the previously documented transcriptional repression of *RBCS* in mesophyll cells is responsible for repressing LS synthesis in mesophyll chloroplasts, a ubiquitin promoter-driven *RBCS* gene was expressed in both bundle sheath and mesophyll cells. This did not lead to Rubisco accumulation in the mesophyll, suggesting that LS synthesis is impeded even in the presence of ectopic SS expression. To attempt to bypass this putative mechanism, a ubiquitin promoter-driven nuclear version of the *rbcL* gene was created, encoding an epitope-tagged LS, which was expressed in the presence or absence of the *Ubi-RBCS* construct. Both transgenes were robustly expressed, and the tagged LS was readily incorporated into Rubisco complexes. However, neither immunolocalization nor biochemical approaches revealed significant accumulation of Rubisco in mesophyll cells, suggesting a continuing cell type-specific impairment of its assembly or stability. We conclude that additional cell type-specific factors limit Rubisco expression to bundle sheath chloroplasts.

INTRODUCTION

C4 photosynthesis is characterized by an increased CO_2 assimilation efficiency of Ribulose-1,5-bisphospate carboxylase (Rubisco), which improves plant production under stress conditions such as water limitation (Ghannoum 2009). One defining character of C4 plants such as maize is the cell type-specificity of Rubisco. In maize, the primary fixation of inorganic carbon (as HCO_3) takes place in mesophyll (M) chloroplasts, through its incorporation into the C4 precursor oxaloacetate by phosphoenolpyruvate carboxylase, which is followed by a reduction into malate by malate dehydrogenase (MDH). Malate is transported to bundle sheath (BS) chloroplasts and decarboxylated by malic enzyme (ME) to release NADPH and CO_2, the latter of which is used for secondary carbon fixation by Rubisco into sugar precursors. The C4 pathway depends on the strict localization of Rubisco to BS chloroplasts, a process that occurs during the differentiation of basal C3 cells into dimorphic C4 cells in dicot plants, and is mainly triggered by light-induced differentiation in maize (reviewed in Patel and Berry 2008). Ultimately, Rubisco expression is promoted in BS cells and repressed in M cells.

Higher plant Rubisco is a hexadecamer composed of eight chloroplast-encoded large subunits (LS) and eight nucleus-encoded small subunits (SS). LS is encoded by the *rbcL* gene and SS by the *RBCS* gene family, which in maize includes two members strongly expressed in similar patterns, *RBCS1* and *RBCS2* (Ewing *et al.* 1998), as well as a probable minor member in terms of its expression (Sheen and Bogorad 1986). The light and tissue-specific regulation of *RBCS* and other Rubisco-related genes has been reviewed in detail (Patel and Berry 2008). In maize, *rbcL* is expressed in both M and BS cells in the dark, but upon illumination rapidly becomes BS-specific (Sheen and Bogorad 1985). Since in green tissues of maize *rbcL* is transcribed in both cell types (Kubicki *et al.* 1994), RNA stability regulation is likely to contribute to its cell type specificity, as it does in C4 Amaranth (Boinski *et al.* 1993).

RBCS transcripts are also restricted to BS cells in light-grown maize (Sheen and Bogorad 1986, Sheen and Bogorad 1987). Transient expression assays revealed that both promoter and 3' UTR elements confer this specificity (Viret *et al.* 1994), and a stably transformed maize transgene consisting of the *RBCS* promoter, 5' UTR, transit peptide and 3' UTR, fused to a maize codon-optimized yellow fluorescent protein coding region, is expressed in BS but not M chloroplasts (Sattarzadeh *et al.* 2010). Both the 5' and 3' UTRs of one *RBCS* family member, *RBCS-m3*, have binding sites for TRM1, a zinc-finger protein that may repress *RBCS*

expression in M cells, although *TRM1* expression itself does not appear to be cell type-specific (Xu *et al.* 2001).

Whatever the underlying mechanism, repression of SS transcription in M cells would be sufficient, in principle, to assure cell type specificity of Rubisco accumulation. Furthermore, we have previously shown using tobacco that in the absence of SS, LS is subject to translational repression, most likely through an interaction of unassembled LS with its encoding *rbcL* transcript (Wostrikoff and Stern 2007). If this occurs in maize, it would coordinate the repression of SS and LS synthesis. In the current study, we test whether LS is indeed subject to translational repression in M cells, and attempt to overcome both SS and LS repression in the M using a transgenic approach. The results show that additional barriers exist to Rubisco accumulation, perhaps at the level of Rubisco complex assembly.

RESULTS

LS is a CES subunit in maize

It is known that Rubisco LS translation is inhibited in the absence of SS in both algae and tobacco (Khrebtukova and Spreitzer 1996, Rodermel *et al.* 1996). In tobacco, it was shown that this translational repression is an autoregulatory mechanism called CES (control by epistasy of synthesis), mediated by residual unassembled LS (Wostrikoff and Stern 2007). We reasoned that the previously documented down-regulation of *RBCS* transcription in M cells (Viret *et al.* 1994) could similarly result in decreased LS translation in M cells. Indeed, a reduced LS translation rate in maize M vs. BS cells has previously been observed using *in organello* pulse labeling (Meierhoff and Westhoff 1993). *rbcL* mRNA accumulation is also decreased in M cells (Langdale *et al.* 1988a), perhaps as a consequence of decreased translation.

To confirm these data, we separated M and BS cells, isolated RNA, and used gel blot analysis and qRT-PCR to gauge mRNA abundance (Figure 1A). As expected, these analyses showed that both *RBCS* and *rbcL* mRNAs accumulated to much higher levels in the BS. In addition, *RBCS* transcripts were barely detectable in M cells, whereas *rbcL* transcripts accumulated to about 30% of the level observed in BS extracts. As controls for cell type cross-contamination, *MDH* was used as a M-specific transcript, and *ME* as a BS-enriched transcript, and their levels were normalized to the validated control Membrane Protein P1A10.07c (Manoli *et al.* 2012), which is similarly expressed in BS and M cells based on Laser Capture Microdissection (LCM) (Li *et al.* 2010). The M to BS ratio was found to average 3% for *ME* and 435% for *MDH* (Figure

1C, data not shown), levels that compare to the LCM values of 11% and 475%, respectively. This shows that for M cell purification, the protoplast isolation method yields extracts with low cross-contamination.

To test the translational status of *rbcL* mRNA, polysome analysis was performed. Extracts from M protoplasts or total cellular material were sedimented through sucrose gradients under native conditions, where ribosome association with transcripts is preserved. The sedimentation rates of RNAs will generally be proportional to their mass, thus reflecting the number of ribosomes bound to each message. To assess the translational status of a given RNA, its distribution pattern across the gradient is determined through the isolation of heavy to light fractions, with untranslated RNA remaining in the lighter, nonpolysomal fractions.

Figure 1B shows distribution patterns of *rbcL and a* control chloroplast mRNA, *psaB*. While the profile for *psaB* was similar in M and total (TS) RNA samples, the *rbcL* hybridization signal was not only weaker in M polysomes, reflecting its decreased abundance, but its distribution also differed as the mRNA was concentrated near the top of the gradient, and thus not engaged in translation. Therefore, in M cells, where *RBCS* is poorly transcribed, *rbcL* mRNA is poorly translated. These data are consistent with the interpretation that Rubisco LS is a CES protein in maize, as it is in tobacco and Chlamydomonas.

To test the correlation between *RBCS* expression and LS translation with an independent method, we first tried to identify mutations in the maize *RBCS1* and *RBCS2* genes by PCR-based screening of the Photosynthetic Mutant Library (http://pml.uoregon.edu/photosyntheticml.html). However, this approach was unsuccessful. We then created an RNAi construct, ZmsiSS, designed to silence all the endogenous *RBCS* genes, as diagramed in Figure 2A. Regeneration of six independent events from *Agrobacterium*-mediated transformation yielded multiple pale-green plantlets that could be maintained *in vitro* on medium supplemented with sucrose, as well as WT-appearing plants.

Seven plantlets were shown by PCR to have integrated the full silencing cassette (data not shown) and were further characterized. Three of them showed the pale-green phenotype typically observed in Rubisco-deficient mutants such as *bsd2*, while the remaining four appeared as the WT. RT-PCR was conducted using primers that would amplify both *RBCS1* and *RBCS2* cDNAs. As exemplified in Figure 2B, green plantlets (“control”) had normal *RBCS*

transcript accumulation, whereas ZmsiSS pale-green plantlets displayed strongly reduced *RBCS* transcript accumulation. The reduced *RBCS* transcript accumulation was correlated with Rubisco deficiency, as revealed by the immunoblot shown in Figure 2C. Figures 2B and C present the characterization of one of three ZmsiSS pale-green transgenics with similar expression data, along with an unsilenced plantlet.

We next investigated the translational status of the *rbcL* transcript in the silenced lines by polysome analysis. The results depicted in Figure 3 show a shift in *rbcL* transcript polysome association when the ZmsiSS line is compared to the unsilenced control. In ZmsiSS the transcript is mostly nonpolysomal and found in fractions 3-6, whereas the largest peak of *rbcL* mRNA in the unsilenced control is found in fractions 8-10. This indicates that maize LS is, as in tobacco and Chlamydomonas, a CES subunit, whose translation is controlled by its assembly state: In the absence of SS, LS translation is decreased.

Steps limiting Rubisco accumulation in M cells: a working hypothesis

The data shown in Figures 1-3, along with previously published results, led us to formulate a working model for differential Rubisco accumulation in BS versus M cells (Fig. 4). In M cells, *RBCS* transcription is down-regulated, leading to the absence of SS in M chloroplasts. LS, being a CES subunit, therefore represses its own synthesis. We hypothesized that down-regulation of LS synthesis leads to *rbcL* transcript destabilization, thereby accounting for limited *rbcL* mRNA accumulation in M cells (see Figure 1A). In BS cells, *RBCS* is expressed, avoiding any repression of LS synthesis. The model in Figure 4 assumes no differential presence of Rubisco chaperones in the two cell types, allowing us to derive several experimentally testable predictions. First, this model assumes that the primary control over differential Rubisco accumulation is through the transcriptional regulation of *RBCS*. Second, the model assumes that there is a link between *rbcL* transcript stability and translational status. We then set out to test these two predictions.

Ectopic expression of SS does not lead to Rubisco accumulation in M cells

According to our working model, the repression of *RBCS* transcription could alone be responsible for the lack of Rubisco accumulation in M cells. To test this, we decided to force *RBCS* transcription in M cells. If the model were correct, the presence of SS in M cells should de-repress LS translation, leading to *rbcL* transcript stabilization. Availability of both LS and SS

should then result in Rubisco assembly and accumulation, assuming all necessary chaperones were present.

To create an appropriate transformation cassette, we relied on previous work which had established, using transient assays, the *RBCS cis* elements that are required for transcriptional repression in the M (Viret *et al.* 1994). This work suggested that both promoter/5' UTR and 3' UTR elements contributed to this regulation. We therefore replaced both these elements to generate the UbiSSnos construct shown in Figure 5A. This chimeric gene includes the native *RBCS* coding region and chloroplast transit peptide, driven by the ubiquitin promoter, flanked by the *nos* 3' UTR. We have previously used the *UBI-nos* combination to drive a *RBCS* transit peptide-*yfp* fusion, which was expressed in all leaf cells (Sattarzadeh *et al.* 2010).

UbiSSnos transformants were generated, and qRT-PCR results from a representative experiment are shown in Figure 5B. We found that the UbiSSnos transgene transcripts accumulated in both M and BS preparations, with no signal as expected in the untransformed control (WT). When primers were used that amplify collectively all *RBCS* transcripts (*RBCS*), expression was limited to the BS in WT, but occurred in both cell types in the transgenic. Primers specific for the endogenous *RBCS1* gene showed BS-restricted expression in both genotypes (data not shown). As control, cross-contamination level of the M extracts by BS was assessed by the M to BS ratio of *ME* transcript. A low level, similar in both WT and UbiSS lines, was observed, indicating that the transgene indeed is expressed in M cells, and was not detected in M preparations as the result of cross-contamination. Thus, the transgene engendered cell type-independent expression of *RBCS* mRNA.

We then analyzed the accumulation of Rubisco using anti-LS and anti-SS antibodies (Fig. 5C). As expected, LS and SS were abundant in both BS samples. In the WT control, some LS signal was seen in the M sample, resulting from contamination by BS proteins and possibly weak Rubisco expression in M cells, as suggested by the relatively high *rbcL* transcript accumulation, which is higher than the cross-contamination level (Figure 1A). The profile was indistinguishable in the transgenic sample, where the M cross-contamination by BS protein was estimated to be similar to the WT, as gauged by the BS-specific ME marker. This suggests that Rubisco does not accumulate to a significant level in UbiSSnos M chloroplasts even though the *RBCS* transcript accumulates. To assess whether the ectopically-expressed *RBCS* mRNA is translated, we used gel blots to assess *UbiSSnos* transcript distribution on M polysomes, using

an *RBCS* probe that detects both native and transgenic *RBCS* sequences. Figure 5D shows that *RBCS* mRNA is polysome-associated in transgenic M samples. The absence of an *RBCS* hybridization signal in WT M polysomes (data not shown) allows us to attribute the signal observed in M transgenic cells to the *UbiSSnos* transgene. The lack of a detectable amount of SS protein in M cells can therefore be attributed to a defect in Rubisco assembly, as it is known that unassembled SS undergoes rapid proteolysis (Schmidt and Mishkind 1983). Taken together, these results demonstrate that strong expression of SS on the transcriptional level in M cells is insufficient to promote stable Rubisco accumulation. Moreover, *RBCS* expression did not induce LS translation, as the distribution of the *rbcL* transcript in polysome analysis was similar in the UbiSSnos transgenic line as compared to the WT; nor did it have a consequence on *rbcL* transcript stability (data not shown). Our working model was thereby refuted.

Recoding and expression of LS as a nuclear gene product

Since ectopic expression of *RBCS* in M cells did not lead to Rubisco accumulation, we considered other negative regulatory mechanisms that might need to be overcome. Two obvious candidates were repression of LS translation, and/or an inability to fold LS in M chloroplasts. As documented above, *rbcL* mRNA is of low abundance and poorly translated in M cells, and M expression of the *UbiSSnos* transcript did not alter this (data not shown). Failed LS folding would be possible if a key chaperone were not present in the M. The one reported Rubisco-specific chaperone, BSD2, however, is found in both cell types (Friso *et al.* 2010).

If either translational repression or protein folding were problematic, they could in principle be overcome by expressing LS from the nucleus, where RNA stability regulation would likely be cell type-independent, and where the protein would be expected to be normally refolded after chloroplast import via the same machinery that imports and refolds SS and many other proteins. To create the appropriate LS expression cassette, *rbcL* was recoded as a nuclear gene with the appropriate codon bias, and named *RBCL*$_N$. A Flag epitope tag was added at the C-terminus, to enable distinction between LS of nuclear origin and chloroplast-encoded LS. This chimeric coding region was then put in the same context as the UbiSSnos transgene, i.e. flanked by the ubiquitin promoter, SS transit peptide, and *nos* terminator (Fig. 6A; UbiLS$_N$nos). In a second transgenic line, UbiLS$_N$nos was introduced along with UbiSSnos, creating plants that expressed both LS and SS under control of the ubiquitin promoter (Fig. 6A; UbiSS-LS$_N$).

We analyzed the double transformants to address the key issue of whether nucleus-encoded LS could be properly imported into chloroplasts, and incorporated into Rubisco. This was tested by immunoblot analysis of total stromal proteins extracted under native conditions, using either an anti-LS antibody, or an anti-Flag antibody for the nucleus-encoded version. As shown in Figure 6B (left panel), Rubisco is the dominant stained band. The center panel shows that total Rubisco migrated at the same position as this stained band, which represents the 550 kD hexadecamer. The quantity did not seem to differ substantially between the WT control and UbiSS-LS_N, a conclusion which is further substantiated below. When the anti-Flag antibody was used (right panel); the control showed two faint cross-reacting bands, one of it at the size of the Rubisco holoenzyme. However a strong signal was seen for the transgenic, as expected. In addition, all of the signal was at the position of assembled Rubisco. While we cannot exclude that some amount of nucleus-encoded LS is subject to proteolysis, either because it does not enter the chloroplast, or because it does not fold correctly after import, these data demonstrate that nucleus-encoded LS can assemble into presumably functional Rubisco. A similar conclusion was reached in an earlier study where LS was expressed from the nucleus in tobacco (Kanevski and Maliga 1994).

Localization and expression of nucleus-encoded LS

The immunoblot data in Figure 6 indicated that nucleus-encoded LS assembles into Rubisco. To see whether any of this Rubisco was in M cells, we examined the double transformant UbiSS-LS_N, reasoning that without *RBCS* expression in M cells, Rubisco accumulation would certainly not occur. Mesophyll RNA preparations were made from the WT and transformant and analyzed by qRT-PCR, as exemplified in Figure 7A. This analysis showed that both SS and LS transgenes were expressed at the RNA level in M cells, well above the cross-contamination level as assessed by *ME* quantification. Next, we used immunoblot analysis to explore whether the product of the nuclear LS gene was present in M cells (Fig. 7B). To judge cross-contamination between M and BS proteins, PEPC was used as a M-specific protein, and ME and Rubisco activase (RCA) as BS-enriched markers. After accounting for differential loading based on the AtpB immunoblot, representing a chloroplast protein whose accumulation is roughly equal between BS and M (Majeran *et al.* 2008), we concluded that the BS preparations were only slightly contaminated with M proteins, whereas a similar level of BS contamination was found in M preparations from both control and transformant samples. To examine Rubisco we used anti-Flag, anti-LS and anti-SS antibodies. The latter two antibodies detect all Rubisco,

which appeared to exhibit a similar ratio of M to BS signal in the WT and transgenic line. Again the LS M to BS ratio is higher than that of the cross-contamination control ME, suggesting that a small amount of LS does accumulate in M cells, but not in a transgenic-specific manner. As observed in Figure 6, a slight cross-reaction was observed when using the anti-Flag antibody with WT proteins. In Figure 7B, a BS-enriched protein which migrates just above Rubisco LS was immunodecorated in both WT and UbiSS-LS_N samples. As expected though, anti-Flag gave a major signal in the transformant at the position of LS. The ratio of M to BS signal was similar to that seen with anti-LS, suggesting that Flag-tagged LS was predominantly accumulating in BS cells. These and other blots suggested that if LS were accumulating in M cells of the transgenic line, this accumulation was minimal and no different than in the WT.

To ensure that the ectopic transcripts are actively translated in M cells of the double transformant, polysome analysis was performed. A probe directed against the *RbcL*$_N$ transcript gave a signal in polysome-associated transcripts of the M of the UbiSS-LS_N transgenic line (Figure 7C), and the *UbiSSnos* transgene was similarly detected with an *RBCS* probe. This showed that both *RbcL*$_N$ and *UbiSSnos* mRNAs are largely loaded onto polysomes, as was the case for the latter transcript in the single transgenic line (Fig. 5D). These results suggest that both Rubisco subunits are produced in M cells of the double transgenic line, but that Rubisco assembly does not occur.

As an independent approach to detecting Rubisco in M cells, we used immunofluorescence in leaf cross-sections, as shown in Figure 8A. First, an anti-Flag antibody was used to localize nucleus-encoded LS (two left columns). As expected, a strong signal was seen in transgenic material expressing LS_N, corresponding to BS cells. We also noted punctate staining in the M and epidermal layers, however similar staining was seen in the two negative controls (WT and UbiSS). Therefore, these data support the conclusion obtained using immunoblots. We also used an anti-LS antibody to visualize total Rubisco (two right columns). A strong green signal indicated a BS localization, and no obvious staining was seen in M cells.

As an indication of whether nucleus-encoded LS could accumulate in M chloroplasts under any conditions, we analyzed etiolated tissues, in which Rubisco expression is not yet cell type-specific (Langdale *et al.* 1988b). Figure 8B (top row) shows two examples in which the anti-Flag antibody was able to detect LS in a cell type-independent manner in these samples, while no

significant staining was observed in the WT control (Fig. 8B, bottom rows). Thus, the LS_N protein can be imported into M plastids, and is not inherently unstable in this context.

While we were certain that nucleus-encoded LS was being expressed, it was unclear whether Ubi-LS_N expression influenced the overall level of Rubisco accumulation; and whether LS_N constitutes a significant proportion of total Rubisco in the transgenic lines. To address the first question, immunoblot analysis of total protein was performed, as shown in Figures 9A and 9B. When the WT control was set to 100%, the three transgenic lines accumulated 80-100% of this level, as compared to the cytochrome *f* control. Thus, overall Rubisco accumulation is not significantly modified in these lines, in agreement with the result shown for UbiSS-LS_N shown in Figure 6B.

We next used immunoblots to estimate the contribution of Flag-tagged LS to the total Rubisco population. To do this, we used protein standards either for the anti-Flag antibody or for the anti-LS antibody. We compared the signals using known amounts of these standards to several dilutions of total protein from plants expressing either UbiSS-LS_N or Ubi-LS_N. Multiple repetitions were carried out, with representative blots shown in Figure 9C. While it proved difficult to obtain statistically significant data, the results clearly show that LS_N makes a strong contribution to the overall Rubisco population. Based on the Flag and LS standards, we estimate that nucleus-encoded LS represents between 25% and 60% of total LS, depending on the transgenic event and sample analyzed.

In summary, we conclude that both the nuclear and chloroplast versions of *rbcL* are robustly expressed in the transgenic plants, and both are incorporated into Rubisco. This suggests that the C-terminal Flag tag is not detrimental to LS synthesis, import, or assembly. The fact that overall Rubisco levels did not rise in BS chloroplasts suggests that another protein is limiting, presumably either SS or a chaperone, or that homeostasis limits Rubisco accumulation through mechanism(s) which remain to be identified.

DISCUSSION

Overcoming barriers to Rubisco accumulation in the mesophyll

The work presented here describes attempts to engender Rubisco accumulation in maize mesophyll chloroplasts, which normally lack this enzyme. It has long been known that *RBCS* genes are transcriptionally repressed in M cells of light-grown maize (Sheen and Bogorad

1986). In other C4 systems such as *Flaveria* and *Amaranth*, post-transcriptional regulation has also been highlighted, as lack of *RBCS* accumulation in M depends on the UTR of the transcripts (for review see Hibberd and Covshoff 2010, Patel *et al.* 2004, Patel *et al.* 2006). *RBCS* gene expression is then a commonly regulated target to establish C4 Rubisco patterning. The regulator itself has not definitely been determined. While TRM1 remains a candidate, other candidates might be found among the genes differently expressed between closely related C3 and C4 species in recent transcriptomic studies (Brautigam *et al.* 2011, Gowik *et al.* 2011). If *RBCS* transcriptional regulation were the sole regulatory point in maize, bypassing this repression would lead to Rubisco assembly, especially given that *rbcL* mRNA accumulates in M chloroplasts albeit at a reduced level relative to BS (Sheen and Bogorad 1985). Ectopic expression of *RBCS* mRNA, however, did not lead to Rubisco accumulation in M, suggesting that additional regulatory barriers were present.

Whether *RBCS* expression is only one limitation to cell type-specific Rubisco accumulation in other C4 systems, remains to be determined. Nonetheless, regulation of *rbcL* at post-transcriptional levels such as transcript stability and translation, has also been observed in other C4 species including Sorghum (Kubicki *et al.* 1994) and *Amaranth* (Boinski *et al.* 1993). In the case of *Amaranth*, an RNA-binding protein whose binding might be involved in *rbcL* mRNA activation in BS chloroplasts was identified (McCormac *et al.* 2001). Together, this indicates that *rbcL* post-transcriptional regulation is another primary checkpoint in C4 establishment. We therefore expressed LS from the nuclear genome, to bypass *rbcL* mRNA instability and repression of chloroplast LS translation, or the absence of an LS-specific translational activator. While the $RBCL_N$ transgene was expressed at the protein level and this protein could assemble into Rubisco in both BS chloroplasts and etiolated M plastids, no or very little Rubisco accumulated in differentiated M chloroplasts. To the extent that our results with LS can be generalized, they suggest that while ectopic expression of BS genes in M cells is possible, movement of entire pathways between cell types is likely to be challenging. This is particularly likely given that M expression of Rubisco, an enzyme with only two structural genes, could not be achieved..

RBCS expression in mesophyll cells

The basis for the differential expression of *RBCS* transcripts in BS and M cells appears to include multiple mechanisms. Early transient expression assays showed that *RBCS* promoter sequences alone did not confer cell type-specific expression (Bansal *et al.* 1992), and a 3’ UTR

element was subsequently found to be important for transcriptional repression in M cells (Viret *et al.* 1994). Repression requires sequence elements that bind the zinc finger protein TRM1 (Xu *et al.* 2001). Maize *RBCS* also appears to be regulated post-transcriptionally, and examination of *RBCS* cell-type specific expression in other C4 species also suggests both transcriptional and post-transcriptional mechanisms (reviewed in Hibberd and Covshoff 2010). To overcome all of these barriers we placed the SS coding region under the control of alternative promoter and 3' elements, using the ubiquitin promoter that we had previously shown to drive high-level YFP expression in M chloroplasts when YFP was fused to the SS transit peptide (Sattarzadeh *et al.* 2010). This led to strong expression of *RBCS* in M cells (Fig. 5B), with around an 8 to 10-fold enrichment of *RBCS* transcripts in M of the transgenic lines as compared to WT M cells.

Evidence that the ectopically-expressed *RBCS* mRNA is efficiently translated in M cells was obtained through polysome analysis (Figures 5D and 7C). Thus, SS is likely produced in M cells of the transgenic plants. It was more difficult to assess whether SS is imported into M chloroplasts, given its failure to assemble into Rubisco. As mentioned above, however, the SS transit peptide directs import of YFP into M chloroplasts. It is therefore very likely that UbiSS transgenic plants import significant amounts of SS into M chloroplasts, which is degraded due to is failure to assemble (Schmidt and Mishkind 1983). Furthermore, we note that although some earlier studies posited that *RBCS* transcripts might be subject to degradation in the M (reviewed in Hibberd and Covshoff 2010), this is clearly not the case in the case of UbiSS, which lacks the native 3' UTR of *RBCS*. Our results also contrast with those for *ME*, whose BS-specific *cis* element lies within the coding region (Brown *et al.* 2011). Clearly, C4-specific RNA patterns arise through multiple mechanisms, as regulatory targets for transcriptional or post-transcriptional regulation have been found in the promoter region such as the MEM1 element in the Flaveria *PEPC* promoter (Gowik *et al.* 2004), 5' UTR regions of the *Amaranth* and *Flaveria RBCS* genes (Patel *et al.* 2004, Patel *et al.* 2006), and also the coding region (*ME*; Brown *et al.* 2011) and 3' UTR (*RBCS*; Xu *et al.* 2001).

Overcoming barriers to LS accumulation in M chloroplasts

Having determined that SS expression in M cells did not lead to Rubisco accumulation, we considered whether LS was also subject to forms of repression. It is known from several studies where SS expression was down-regulated, that LS and SS accumulation are concerted (Furbank *et al.* 1996, Makino *et al.* 1997, Rodermel *et al.* 1988). One mechanism underlying this phenomenon that has been described in tobacco, is the translational repression of LS in the

absence of its assembly partner (Rodermel *et al.* 1996). Subsequent work showed that this repression acts through the Controlled Epistasy of Synthesis (CES) mechanism, in which unassembled LS is believed to act as an autoregulator (Wostrikoff and Stern 2007). Where such negative autoregulation of chloroplast translation has been dissected in detail, it relies on binding of unassembled proteins, most likely in concert with tertiary effectors, to the 5' UTRs of the targeted mRNAs (Boulouis *et al.* 2011). In maize, *rbcL* mRNA is primarily in nonpolysomal fractions in M chloroplasts (Fig. 1B), consistent with this mechanism and also with earlier results showing that purified M chloroplasts synthesize very low amounts of LS during pulse labeling, as compared to BS chloroplasts (Meierhoff and Westhoff 1993).

To test whether LS is subject to a CES-like mechanism in maize M chloroplasts, we reduced SS expression using RNAi. In these silenced ZmsiSS lines, lacking the SS in both M and BS cells, the *rbcL* profile is comparable to that observed for WT M cells: *rbcL* mRNA is shifted towards the nonpolysomal fractions. We note that these profiles do not completely overlap (compare Fig. 1B and Fig. 3), a phenomenon we tentatively attribute to the fact that the experiment in Figure 1 requires a 3 h incubation to isolate M protoplasts, during which there is likely to be some polysomal run-off. Nevertheless, it is clear from our data that the transgenic lines deficient for SS exhibit translational repression of *rbcL*, a hallmark of a CES subunit. We therefore speculate that reduced *rbcL* M polysomal association in WT cells also results from the inability of LS to assemble. Support for LS autoregulation in the M comes from the *bsd2* mutant phenotype. As shown for tobacco, *bsd2* down-regulation leads to LS instability, which removes the possibility of it repressing its own synthesis in absence of SS (Wostrikoff and Stern 2007). In the maize *bsd2* mutant, *rbcL* mRNA polysome association increases in M cells (Brutnell *et al.* 1999), again suggesting that LS must accumulate to a minimal level in order to mediate translational autoregulation.

Another set of observations incorporated into our hypothesis (Fig. 4), is that translational repression of *rbcL* mRNA leads to its instability. In maize, M-localized *rbcL* mRNA has been shown to be unstable (Kubicki *et al.* 1994), and several maize mutants exhibit a correlation between general translational defects and *rbcL* mRNA instability (Barkan 1993, Schultes *et al.* 2000), the opposite of what was observed with *bsd2*, where in the M, both polysome loading and accumulation of *rbcL* mRNA increased. Our data from ZmsiSS, however, did not show any evidence for *rbcL* mRNA instability when measured in the context of total RNA; M protoplasts could not be isolated due to the fragile nature of the transformants and their lethality.

Furthermore, a 2 h treatment of M protoplasts with lincomycin, which inhibits translation elongation shortly after initiation (Kim *et al.* 1994), did not lead to *rbcL* mRNA instability (data not shown). We conclude that translational status and stability of *rbcL* mRNA are not inextricably linked.

Our strategy for expressing LS in the M was to relocate the gene to the nucleus, after optimizing codon usage. A previous approach in tobacco combined deletion of the *rbcL* gene through chloroplast transformation, with expression of that same sequence under control of nuclear *cis* elements (Kanevski and Maliga 1994). This led to accumulation of approximately 10% of the WT level of Rubisco. Similarly, a *psbA* gene expressed in the nucleus yielded low amounts of protein relative to its endogenous counterpart (Cheung *et al.* 1988). We reasoned that codon optimization might increase the production of nucleus-encoded LS. While we did not compare optimized and non-optimized versions directly, Flag epitope-tagged LS_N was readily detectable, and in various experiments appeared to constitute as much as half of the total LS in transformants (Fig. 9 and data not shown). Furthermore, based on native gel electrophoresis, all accumulating LS_N is incorporated into Rubisco (Fig. 6), suggesting that LS assembly does not require its intraplastidial synthesis. Because we do not know precisely how much LS_N is initially produced, we cannot ascertain the efficiency of its assembly relative to the endogenous protein, nor whether there is any effect of the C-terminal nine amino acid Flag epitope.

Limitations to Rubisco accumulation in maize

Our approach could have led both to ectopic accumulation of Rubisco in M chloroplasts, as well as overaccumulation of Rubisco in BS, where transgenic lines expressed both LS and SS under control of the ubiquitin promoter. Given that Rubisco accounts for only 5-9% of leaf nitrogen in C4 plants (Sage *et al.* 1987), as opposed to a much higher figure in C3 plants (reviewed in Feller *et al.* 2008), N availability would not appear *a priori* to be a limitation to increasing the Rubisco level, especially given that a 30% increase was achieved on a leaf area basis through *RBCS* overexpression in rice (Suzuki *et al.* 2007), which is C3. Our results, however, suggested that none of the transgenic lines accumulated more Rubisco than the WT (Fig. 9B), and in transgenic wheat, Ubi-*RBCS* expression failed to yield increased Rubisco amount (Mitchell *et al.* 2004). On the other hand, we did not initially screen transformants for overexpression; rather, we sought lines with single insertions that correctly expressed the transgenes.

Many explanations are possible for the failure to overaccumulate Rubisco. For example, limiting amounts of one or more chaperones might be responsible, since imported Rubisco subunits would compete for the machinery that re-folds proteins following their translocation into the chloroplast. Alternatively, high Rubisco accumulation could trigger specific proteolytic mechanisms such as those which degrade the enzyme during plant senescence (Feller *et al.* 2008). Limitation of one or more Rubisco-specific chaperones could also be at play, as we propose below to explain the lack of M chloroplast Rubisco accumulation in transgenic lines, The absence of such a dedicated chaperone could either result either from a physiological need to actively prevent Rubisco accumulation in M chloroplasts, or from the absence of evolutionary pressure leading to its loss in M chloroplasts.

In M cells, ectopic expression of LS and SS was clearly insufficient to produce Rubisco accumulation at a level detectable above background, whether analyzed by immunoblot (Fig. 7B) or immunolocalization (Fig. 8A). This suggests either that an active mechanism degrades transiently assembled Rubisco in this cell type, or that the ectopically-expressed subunits cannot assemble into a stable form. While we cannot readily distinguish between these two alternatives, it is important to consider whether known Rubisco assembly factors are present in both M and BS. At the time our studies were underway, the most probable key players in this respect were BSD2 and RBCX. BSD2 is found in both M and BS chloroplasts, and its amount appears to be similar in the two cell types (Friso *et al.* 2010). This raises the question of BSD2 function in M chloroplasts, where it conceivably function as a repressor of Rubisco expression, in contrast to its proposed role in the BS as a co-translational chaperone for LS (Brutnell *et al.* 1999, Roth *et al.* 1996). As a preliminary test of the latter hypothesis, we placed the UbiLS$_N$nos transgene into a *bsd2* mutant background. Our results showed that the nuclear transgene neither rescued the seedling-lethal phenotype of the *bsd2* mutant, nor did it increase the small amount of LS that accumulates in *bsd2* (data not shown). Thus, BSD2 may in fact act post-translationally rather than co-translationally.

RBCX has a demonstrated essential Rubisco assembly function only in certain cyanobacteria (Onizuka *et al.* 2004), and its function in plants is unknown, although the Arabidopsis RBCX proteins can increase solubility of cyanobacterial LS when expressed in *E. coli* (Kolesinski et al. 2011). In maize, the two *RBCX* genes are both expressed in BS and M cells. Transcripts of the more strongly expressed locus, *RBCX2,* are found equally in BS and M, whereas *RBCX1* is

expressed at a two-fold higher level in BS cells, but only 25% as strongly overall as *RBCX2* (Li *et al.* 2010). This suggests that RBCX proteins are present in both cell types.

Very recently, a new candidate has emerged as a limiting factor for Rubisco accumulation in M chloroplasts. This protein, RAF1, was identified from a maize photosynthetic mutant collection, among strains that specifically lack Rubisco (Feiz *et al.*, in preparation). RAF1, as judged by proteomics and transcriptome analysis, is highly enriched in the BS, and mutant analysis suggests that it is required for assembly of LS into multimers, and/or for subsequent assembly of LS and SS. Whether adding ectopic expression of RAF1 to the SS-LS_N transgenic lines would lead to M Rubisco accumulation, is currently being explored.

MATERIALS AND METHODS:

Plant culture

Plants were grown in soil in greenhouse conditions under 16h day, 8h night at 23°C, unless otherwise specified. For some transgenic plants, analyses were performed on material grown *in vitro* on sucrose-containing MSOD medium. Etiolated plants were grown for 10 days in the dark on vermiculite.

Transgenics

Maize transformation was carried as described (Sattarzadeh *et al.* 2010). Transgenic explants were recovered on the basis of paromomycin resistance conferred by the *nptII* gene present in the binary vectors, and confirmed via an nptII ELISA test (Agdia Corp., Elkhart, IN). Primary transformants were backcrossed to a WT, the Hi II transformation recipient in most cases, which is a hybrid between inbreds A188 and B73. F1 transgenic progeny were identified by PCR genotyping on tissue extracted as the first leaf emerged, using a modified CTAB extraction protocol (Ahern *et al.* 2009), with the *RBCS* cod2 and nos RT rev2 primers for the UbiSS construct and NuLS fw2 and NuLS rev2 primer pair for the nucleus-encoded *RBCL* gene, respectively. All primer sequences are given in Supplemental Table S1.

Plant Transformation Constructs

RNAi silencing cassette. A 347 bp fragment of *ZmRBCS1* (ZmGDB accession GRMZM2G140016) was cloned as an inverted repeat separated by the Rice waxy intron in the vector pMCG161 (http://www.chromdb.org/rnai/vector_info.html), and subcloned into the binary vector pPZP212 (Hajdukiewicz *et al.* 1994). As the sequence used is highly homologous to the *ZmRBCS2* sequence (ZmGDB GRMZM2G1113033), it was anticipated to lead to efficient silencing of both *RBCS* genes. Further subcloning introduced the 4.2 kb *Sca*I fragment of the hp*RBCS* plasmid into S*ma*I-digested pZP212, yielding the plasmid pPTN425 used for maize transformation.

Ubi-SS-nos cassette: The complete *ZmRBCS1* coding sequence (677 bp) was amplified from T43 DNA with primers adding respectively *Hin*dIII and *Cla*I restriction sites (*RBCS*1 AUG-HindIII and *RBCS*1 rev ClaI), using Platinium Pfx DNA polymerase and its enhancer solution (Invitrogen, Carlsbad, CA). The PCR product was cloned in the pGemT-easy vector after adding an A overhang by a 10 min incubation at 72°C with Taq polymerase (Promega, Madison, WI) in the *E.coli* strain GM2163 *dam*$^{-}$*dcm*$^{-}$, yielding the *RBCS* HC-pGemT plasmid. Sequencing of the

PCR product revealed a T to A mutation in the intron at position 269. The 272 bp *nos* terminator was amplified from the plasmid pPTN458 (Sattarzadeh *et al.* 2010) using primers adding *Cla*I and *Apa*I restriction sites at its ends (nos-ClaI and nos-ApaI), and inserted into the *Cla*I-*Apa*I-digested *RBCS* HC-pGemT, yielding the plasmid pHCnos. The *RBCS*-nos sequences were further subcloned following *Hin*dIII-*Apa*I digestion of pHCnos and ligation into *Hin*dIII-*Apa*I-digested pBluescript, yielding the plasmid HCnos-pBS. The *RBCS*-nos sequences were placed downstream of the maize ubiquitin promoter (Christensen *et al.* 1992) by subcloning the *Hin*dIII-*Kpn*I fragment of HCnos-pBS into the pUBI4 plasmid, kindly provided by Dr. A.B. Cahoon (Middle Tennessee State Univ.), yielding the plasmid pUbiHCnos. Further subcloning into the binary vector pPZP212yielded the pPTN438 plasmid that was used for maize transformation.

LS_N construct: The maize *rbcL* chloroplast gene (Genbank accession NC001666) was recoded for efficient expression in the maize nuclear genome (Geneart AG, Regensburg, Germany). 5' sequences corresponding to part of the maize *RBCS* sequences encoding SS transit peptide, as well as a *Bam*HI restriction site, and 3' sequences encoding the FLAG epitope and a *Cla*I restriction site were added by PCR using the Zm*RBCS*TP-NuRbcL.F and ZmNuRbcL flag tag.R primers. The *Bam*HI-*Cla*I product was inserted into the pHCNos delta Bam plasmid, obtained after site-directed mutagenesis destroying the *Bam*HI site in the multicloning site using the HCnospBS delta Bam QC1 and QC2 primers (Quickchange mutagenesis, Stratagene, La Jolla, CA), yielding the plasmid *RBCS*TP-NuRbcL-nos. The *Hind*III-*Kpn*I fragment was then excised and inserted into the plasmid pUbi4 (see above), yielding the plasmid Ubi-*RBCS*TP-NuRbcLFlag-nos. Further subcloning into pPZP212 yielded the plasmid pPTN618. To construct pPTN728, the plasmid Ubi-*RBCS*TP-NuRbcLFLAg-nos was further subcloned into pPTN438 plasmid.

M/BS extraction: BS and M extractions were performed on 2 to 5 g of leaves as described (Markelz *et al.* 2003), except that BS strand isolations were carried out entirely at 4°C to minimize degradation. TS represents tissue incubated as for the preparation of M protoplasts but where cellulase and macerase were omitted (mock treatment). Purity of the extracts was tested either by qRT-PCR on isolated RNA, and/or by immunoblot analysis using known transcripts or proteins highly enriched in either fraction. For qRT-PCR, primers designed against the M-enriched malate dehydrogenase gene *MDH* (Zm-qMDH F1 and R1, Genbank accession X16084.1), the BS-enriched malic enzyme mRNA *ME* (ZmqME F1 and R1, Genbank accession J05130.1), and Membrane protein PB1A10.07c (MEP) transcripts were used (ZM-qMEP F1 and

R1, GRMZM2G018103). For protein characterization, anti-PEPC (Agrisera, Sweden), anti-Rubisco activase (a kind gift of Dr. Michael Salvucci, US Arid-Land Agricultural Research Center, Maricopa, AZ), and anti-malic enzyme antibody (a kind gift of Dr. Timothy Nelson, Yale University, CT) were used as markers for M or BS purity.

RNA characterization

Total RNA was extracted from 150 mg of 2nd or 3rd leaves using Tri-Reagent (Molecular Research, Cincinnati, OH), and analyzed by gel blot hybridizations at 65°C using modified (0.1% BSA) Church and Gilbert buffer (Church and Gilbert 1984).The *rbcL, psaB, RBCS, ME, MDH* and $RBCL_N$ probes were PCR products amplified with primers given in Table I.

For classical RT-PCR experiments, the Access RT-PCR system (Promega, Madison, WI) was used for one-step RT-PCR, starting from 100 ng of RNA. Reverse transcription and PCR were conducted as specified, with a reverse transcription step of 45 minutes at 48°C, followed by a 2 min denaturation at 94°C, and the stated number of cycles of 30s at 94°C, 45s at the appropriate annealing temperature, and 30s at 68°C for primer pairs designed to amplify ubiquitin and total *RBCS* cDNA (with the hp*RBCS* cod1 and rev1 primer pair annealing to both *RBCS1* and *RBCS2* cDNAs).

For quantitative RT-PCR, 5 ug of mRNA were treated with DNAse I and purified using the DNA free RNA kit (Zymo Research, Proteigene, France). Subsequently, 2 µg of mRNA were reverse transcribed using random hexamers and Superscript III (Invitrogen, Carlsbad CA) according to the manufacturer's instructions. qRT-PCR was performed using the FastStart SYBR Green Master Mix (Roche) in a 20 µl reaction in the Rotorgene 3000 (Qiagen). Classical 3-step amplification was performed (annealing at 60°C) and fluorescence acquisition was realized at different temperatures depending on the primer used. Data analysis was carried out with the Rotor Gene Q Series software and the Pfaffl method was used for quantification.

Polysomes were prepared by grinding 150 mg of tissue in 1 ml of polysome extraction buffer as described (Barkan 1998), except that centrifugation was performed at 40,000 rpm at 4°C either for 90 min in a SW-50Ti rotor, or for 108 min in an MLS-50 rotor.

Protein characterization

7.5 to 50 µg of proteins, extracted as described (Wostrikoff and Stern 2007) were separated through SDS gels, and blotted onto nitrocellulose or Hybond C membranes (GE Healthcare, WI). Immunodecoration was performed using standard protocols. Antibodies raised against LS (1:50,000 dilution), SS (1:20,000 dilution), PEPC (1:20,000 dilution) were purchased from Agrisera. Anti-cytochrome *f* and anti-ME were used at 1:10,000 dilution, anti-AtpB at a 1:60,000 dilution, and anti-Rubisco activase at a 1:30,000 dilution. Primary antibodies were incubated overnight at 4°C in TBS-Tween 0.1%, and an anti-Rabbit secondary antibody (1:20,000 dilution) was incubated for 1 h. An anti-flag M2 antibody conjugated to horseradish peroxidase was purchased from Sigma (Saint Louis, MI) and used at a 1:40,000 dilution. The reaction was revealed using the enhanced chemiluminescence kit (Amersham, Pitscataway, NJ) either on X-ray film or using a CCD imaging system (Chemidoc, Biorad).

Immunolocalization:

Thin cross-sections were manually made and fixed in 4% formaldehyde, 5% DMSO and 1X PME for 2 hours, as adapted from a published method (Harrison *et al.* 2002). Vacuum was applied for the first hour of incubation. Sections were secured on cover slips with 0.75% agarose, and treated for 20 minutes with cellulytic enzymes (cellulase RS 1%, pectolyase 0.01%, Phytotechlab, Shawnee Mission, KS) and BSA 0.1% in 1X PME buffer. After 3 washes with 1X PBS, the sections were saturated with 1% BSA in 1XPBS for 90 min.

The anti-flag (F1804, Sigma, St Louis, MO) and anti-LS were added, and incubation was carried out with respectively 1:400 and 1:1,000 dilutions overnight at room temperature in a humid chamber. After 1X PBS washes, secondary antibodies - an AlexaFluor 594 goat anti-mouse antibody for flag detection (A21125) and an AlexaFluor 488 goat anti-rabbit antibody (A11008) for Rubisco detection (Molecular Probes, Invitrogen, Carlsbad, CA) - were incubated at a 1:100 dilution for 2 h in a humid chamber. After washes in 1X PBS, sections were mounted in Mowiol's medium.

Images were collected on a Leica TCS-SP5 confocal microscope (Leica Microsystems, Exton, PA USA) at the BTI Plant Cell Imaging Center using a HCX PL APO CS 40.0x1.25 oil UVimmersion objective, zoom 1.7. For Rubisco immunolocalization, AF488 and chlorophyll autofluorescence were excited with a blue argon ion laser (488 nm), and emitted light was collected for channel 1 between 498 nm and 517 nm, and for channel 2 between 659 nm and 740 nm. For Flag immunolocalization, AF594 was excited with an orange He-Ne laser (594 nm),

and emitted light was collected from 616 nm to 634 nm to minimize chlorophyll autofluorescence. DIC (differential interference contrast) or brightfield images were collected simultaneously using the transmitted light detector and were overlaid with the fluorescence images to reveal the shape of the cross-section. Images were processed using Leica LAS-AF software (version 1.8.2) and Adobe Photoshop CS2 version 9.0.2.

ACKNOWLEDGEMENTS

We thank the ABRC for supplying the pMCG161 plasmid (CD3-459), Dr. Bruce Cahoon (Middle Tennessee State University) for providing pUbi4, Geneart AG (Regensburg, Germany) for synthesis of the nuclear encoded *rbcL* gene, Nicole Markelz and Tom Brutnell (BTI) for help with mesophyll and bundle sheath extraction, and for the *MDH*, *ME*, *UBI*, and *RBCS2* primer sequences, Suzanne Belcher and Alice Barkan (University of Oregon) for attempting a reverse genetic screen for *RBCS* mutants. Dr. Mike Salvucci (USDA, Arizona), and Drs. Tim Nelson and Lori Tausta (Yale University, Connecticut) are gratefully acknowledged for sharing and distributing respectively the RCA and ME antibodies. We thank the BTI Plant Cell Imaging Center for assistance with confocal microscopy.

LITERATURE CITED

Ahern, K.R., Deewatthanawong, P., Schares, J., Muszynski, M., Weeks, R., Vollbrecht, E., Duvick, J., Brendel, V.P. and Brutnell, T.P. (2009) Regional mutagenesis using Dissociation in maize. *Methods*, **49**, 248-254.

Bansal, K.C., Viret, J.F., Haley, J., Khan, B.M., Schantz, R. and Bogorad, L. (1992) Transient expression from cab-m1 and rbcS-m3 promoter sequences is different in mesophyll and bundle sheath cells in maize leaves. *Proc. Natl. Acad. Sci. USA*, **89**, 3654-3658.

Barkan, A. (1993) Nuclear mutants of maize with defects in chloroplast polysome assembly have altered chloroplast RNA metabolism. *Plant Cell*, **5**, 389-402.

Barkan, A. (1998) Approaches to investigating nuclear genes that function in chloroplast biogenesis in land plants. *Meths. Enzymol.*, **297**, 38-57.

Boinski, J.J., Wang, J.L., Xu, P., Hotchkiss, T. and Berry, J.O. (1993) Post-transcriptional control of cell type-specific gene expression in bundle sheath and mesophyll chloroplasts of *Amaranthus hypochondriacus*. *Plant Mol. Biol.*, **22**, 397-410.

Boulouis, A., Raynaud, C., Bujaldon, S., Aznar, A., Wollman, F.A. and Choquet, Y. (2011) The nucleus-encoded trans-acting factor MCA1 plays a critical role in the regulation of cytochrome f synthesis in *Chlamydomonas* chloroplasts. *Plant Cell*, **23**, 333-349.

Brautigam, A., Kajala, K., Wullenweber, J., Sommer, M., Gagneul, D., Weber, K.L., Carr, K.M., Gowik, U., Mass, J., Lercher, M.J., Westhoff, P., Hibberd, J.M. and Weber, A.P. (2011) An mRNA blueprint for C4 photosynthesis derived from comparative transcriptomics of closely related C3 and C4 species. *Plant Physiol.*, **155**, 142-156.

Brown, N.J., Newell, C.A., Stanley, S., Chen, J.E., Perrin, A.J., Kajala, K. and Hibberd, J.M. (2011) Independent and parallel recruitment of preexisting mechanisms underlying C photosynthesis. *Science*, **331**, 1436-1439.

Brutnell, T.P., Sawers, R.J., Mant, A. and Langdale, J.A. (1999) BUNDLE SHEATH DEFECTIVE2, a novel protein required for post- translational regulation of the *rbcL* gene of maize. *Plant Cell*, **11**, 849-864.

Cheung, A.Y., Bogorad, L., Van Montagu, M. and Schell, J. (1988) Relocating a gene for herbicide tolerance: A chloroplast gene is converted into a nuclear gene. *Proc. Natl. Acad. Sci. USA*, **85**, 391-395.

Christensen, A.H., Sharrock, R.A. and Quail, P.H. (1992) Maize polyubiquitin genes: structure, thermal perturbation of expression and transcript splicing, and promoter activity following transfer to protoplasts by electroporation. *Plant Mol. Biol.*, **18**, 675-689.

Church, G. and Gilbert, W. (1984) Genomic sequencing. *Proc. Natl. Acad. Sci. USA*, **81**, 1991-1995.

Ewing, R.M., Jenkins, G.I. and Langdale, J.A. (1998) Transcripts of maize *RbcS* genes accumulate differentially in C3 and C4 tissues. *Plant Mol. Biol.*, **36**, 593-599.

Feller, U., Anders, I. and Mae, T. (2008) Rubiscolytics: fate of Rubisco after its enzymatic function in a cell is terminated. *J. Exp. Bot.*, **59**, 1615-1624.

Friso, G., Majeran, W., Huang, M., Sun, Q. and van Wijk, K.J. (2010) Reconstruction of metabolic pathways, protein expression, and homeostasis machineries across maize bundle sheath and mesophyll chloroplasts: large-scale quantitative proteomics using the first maize genome assembly. *Plant Physiol*, **152**, 1219-1250.

Furbank, R.T., Chitty, J.A., Von Caemmerer, S. and Jenkins, C. (1996) Antisense RNA inhibition of *RbcS* gene expression reduces Rubisco level and photosynthesis in the C_4 plant *Flaveria bidentis*. *Plant Physiol.*, **111**, 725-734.

Ghannoum, O. (2009) C_4 photosynthesis and water stress. *Ann Bot*, **103**, 635-644.

Gowik, U., Brautigam, A., Weber, K.L., Weber, A.P. and Westhoff, P. (2011) Evolution of C4 photosynthesis in the genus *Flaveria*: how many and which genes does it take to make C4? *Plant Cell*, **23**, 2087-2105.

Gowik, U., Burscheidt, J., Akyildiz, M., Schlue, U., Koczor, M., Streubel, M. and Westhoff, P. (2004) *cis*-Regulatory elements for mesophyll-specific gene expression in the C4 plant *Flaveria trinervia*, the promoter of the C4 phosphoenolpyruvate carboxylase gene. *Plant Cell*, **16**, 1077-1090.

Hajdukiewicz, P., Svab, Z. and Maliga, P. (1994) The small, versatile pPZP family of *Agrobacterium* binary vectors for plant transformation. *Plant Mol. Biol.*, **25**, 989-994.

Harrison, M.J., Dewbre, G.R. and Liu, J. (2002) A phosphate transporter from *Medicago truncatula i*nvolved in the acquisition of phosphate released by arbuscular mycorrhizal fungi. *Plant Cell*, **14**, 2413-2429.

Hibberd, J.M. and Covshoff, S. (2010) The regulation of gene expression required for C_4 photosynthesis. *Annu. Rev. Plant Biol.*, **61**, 181-207.

Kanevski, I. and Maliga, P. (1994) Relocation of the plastid *rbcL* gene to the nucleus yields functional ribulose-1,5-bisphosphate carboxylase in tobacco chloroplasts. *Proc. Natl. Acad. Sci. USA*, **91**, 1969-1973.

Khrebtukova, I. and Spreitzer, R.J. (1996) Elimination of the *Chlamydomonas* gene family that encodes the small subunit of ribulose-1,5-bisphosphate carboxylase/oxygenase. *Proc. Natl. Acad. Sci. USA*, **93**, 13689-13693.

Kim, J., Eichacker, L.A., Rudiger, W. and Mullet, J.E. (1994) Chlorophyll regulates accumulation of the plastid-encoded chlorophyll proteins P700 and D1 by increasing apoprotein stability. *Plant Physiol.*, **104**, 907-916.

Kolesinski, P., Piechota, J. and Szczepaniak, A. (2011) Initial characteristics of *RbcX* proteins from *Arabidopsis thaliana*. *Plant Mol. Biol.*, **77**, 447-459.

Kubicki, A., Steinmuller, K. and Westhoff, P. (1994) Differential transcription of plastome-encoded genes in the mesophyll and bundle-sheath chloroplasts of the monocotyledonous NADP-malic enzyme-type C4 plants maize and Sorghum. *Plant Mol. Biol..* **25**, 669-679.

Langdale, J.A., Rothermel, B.A. and Nelson, T. (1988a) Cellular pattern of photosynthetic gene expression in developing maize leaves. *Genes Dev.*, **2**, 106-115.

Langdale, J.A., Zelitch, I., Miller, E. and Nelson, T. (1988b) Cell position and light influence C4 versus C3 patterns of photosynthetic gene expression in maize. *EMBO J.*, **7**, 3643-3651.

Li, P., Ponnala, L., Gandotra, N., Wang, L., Si, Y., Tausta, S.L., Kebrom, T.H., Provart, N., Patel, R., Myers, C.R., Reidel, E.J., Turgeon, R., Liu, P., Sun, Q., Nelson, T. and Brutnell, T.P. (2010) The developmental dynamics of the maize leaf transcriptome. *Nat. Genet.*, **42**, 1060-1067.

Majeran, W., Zybailov, B., Ytterberg, A.J., Dunsmore, J., Sun, Q. and van Wijk, K.J. (2008) Consequences of C4 differentiation for chloroplast membrane proteomes in maize mesophyll and bundle sheath cells. *Mol. Cell. Proteomics*, **7**, 1609-1638.

Makino, A., Shimada, T., Takumi, S., Kaneko, K., Matsuoka, M., Shimamoto, K., Nakano, H., Miyao-Tokutomi, M., Mae, T. and Yamamoto, N. (1997) Does decrease in Ribulose-1,5-bisphosphate carboxylase by antisense *RbcS* lead to a higher N-use efficiency of photosynthesis under conditions of saturating CO_2 and light in rice plants? *Plant Physiol.*, **114**, 483-491.

Manoli, A., Sturaro, A., Trevisan, S., Quaggiotti, S. and Nonis, A. (2012) Evaluation of candidate reference genes for qRT-PCR in maize. *J. Plant Physiol.*, **169**, 807-815.

Markelz, N.H., Costich, D.E. and Brutnell, T.P. (2003) Photomorphogenic responses in maize seedling development. *Plant Physiol.*, **133**, 1578-1591.

McCormac, D.J., Litz, H., Wang, J., Gollnick, P.D. and Berry, J.O. (2001) Light-associated and processing-dependent protein binding to 5′ Regions of *rbcL* mRNA in the chloroplasts of a C4 plant. *J. Biol. Chem.*, **276**, 3476-3483.

Meierhoff, K. and Westhoff, P. (1993) Differential biogenesis of photosystem II in mesophyll and bundle-sheath cells of monocotyledonous NADP-malic enzyme-type C_4 plants: the non-stoichiometric abundance of the subunits of photosystem II in the bundle-sheath chloroplasts and the translational activity of the plastome-encoded genes. *Planta*, **191**, 23-33.

Mitchell, R.A.C., Joyce, P.A., Rong, H., Evans, V.J., Madgwick, P.J. and Parry, M.A.J. (2004) Loss of decreased-rubisco phenotype between generations of wheat transformed with antisense and sense *rbcS*. *Ann. appl. Biol.*, **145**, 209-216.

Onizuka, T., Endo, S., Akiyama, H., Kanai, S., Hirano, M., Yokota, A., Tanaka, S. and Miyasaka, H. (2004) The *rbcX* gene product promotes the production and assembly of ribulose-1,5-bisphosphate carboxylase/oxygenase of *Synechococcus* sp. PCC7002 in *Escherichia coli*. *Plant Cell Physiol.*, **45**, 1390-1395.

Patel, M. and Berry, J.O. (2008) Rubisco gene expression in C4 plants. *J .Exp. Bot.*, **59**, 1625-1634.

Patel, M., Corey, A.C., Yin, L.P., Ali, S., Taylor, W.C. and Berry, J.O. (2004) Untranslated regions from C_4 *Amaranth AhRbcS1* mRNAs confer translational enhancement and preferential bundle sheath cell expression in transgenic C_4 *Flaveria bidentis*. *Plant Physiol.*, **136**, 3550-3361.

Patel, M., Siegel, A.J. and Berry, J.O. (2006) Untranslated regions of *FbRbcS1* mRNA mediate bundle sheath cell-specific gene expression in leaves of a C4 plant. *J. Biol. Chem.*, **281**, 25485-25491.

Rodermel, S., Haley, J., Jiang, C.Z., Tsai, C.H. and Bogorad, L. (1996) A mechanism for intergenomic integration: abundance of ribulose bisphosphate carboxylase small-subunit

protein influences the translation of the large-subunit mRNA. *Proc. Natl. Acad. Sci. USA.*, **93**, 3881-3885.

Rodermel, S.R., Abbott, M.S. and Bogorad, L. (1988) Nuclear-organelle interactions: nuclear antisense gene inhibits ribulose bisphosphate carboxylase enzyme levels in transformed tobacco plants. *Cell*, **55**, 673-681.

Roth, R., Hall, L.N., Brutnell, T.P. and Langdale, J.A. (1996) *bundle sheath defective2*, a mutation that disrupts the coordinated development of bundle sheath and mesophyll cells in the maize leaf. *Plant Cell*, **8**, 915-927.

Sage, R.F., Pearcy, R.W. and Seemann, J.R. (1987) The nitrogen use efficiency of C(3) and C(4) plants : III. Leaf nitrogen effects on the activity of carboxylating enzymes in *Chenopodium album* (L.) and *Amaranthus retroflexus* (L.). *Plant Physiol.*, **85**, 355-359.

Sattarzadeh, A., Fuller, J., Moguel, S., Wostrikoff, K., Sato, S., Covshoff, S., Clemente, T., Hanson, M. and Stern, D.B. (2010) Transgenic maize lines with cell-type specific expression of fluorescent proteins in plastids. *Plant Biotechnol. J.*, **8**, 112-125.

Schmidt, G.W. and Mishkind, M.L. (1983) Rapid degradation of unassembled ribulose 1,5-bisphosphate carboxylase small subunits in chloroplasts. *Proc. Natl. Acad. Sci. USA*, **80**, 2632-2636.

Schultes, N.P., Sawers, R.J., Brutnell, T.P. and Krueger, R.W. (2000) Maize high chlorophyll fluorescent 60 mutation is caused by an Ac disruption of the gene encoding the chloroplast ribosomal small subunit protein 17. *Plant J.*, **21**, 317-327.

Sheen, J.Y. and Bogorad, L. (1985) Differential expression of the ribulose bisphosphate carboxylase large subunit gene in bundle sheath and mesophyll cells of developing maize leaves is influenced by light. *Plant Physiol.*, **79**, 1072-1076.

Sheen, J.Y. and Bogorad, L. (1986) Expression of the ribulose-1,5-bisphosphate carboxylase large subunit gene and three small subunit genes in two cell types of maize leaves. *EMBO J.*, **5**, 3417-3422.

Sheen, J.Y. and Bogorad, L. (1987) Differential expression of C4 pathway genes in mesophyll and bundle sheath cells of greening maize leaves. *J. Biol. Chem.*, **262**, 11726-11730.

Suzuki, Y., Ohkubo, M., Hatakeyama, H., Ohashi, K., Yoshizawa, R., Kojima, S., Hayakawa, T., Yamaya, T., Mae, T. and Makino, A. (2007) Increased Rubisco content in transgenic rice transformed with the 'sense' *rbcS* gene. *Plant Cell Physiol.*, **48**, 626-637.

Viret, J.F., Mabrouk, Y. and Bogorad, L. (1994) Transcriptional photoregulation of cell-type-preferred expression of maize *RBCS-m3*: 3' and 5' sequences are involved. *Proc. Natl. Acad. Sci. USA*, **91**, 8577-8581.

Wostrikoff, K. and Stern, D. (2007) Rubisco large-subunit translation is autoregulated in response to its assembly state in tobacco chloroplasts. *Proc. Natl. Acad. Sci. USA*, **104**, 6466-6471.

Xu, T., Purcell, M., Zucchi, P., Helentjaris, T. and Bogorad, L. (2001) TRM1, a YY1-like suppressor of *RBCS-m3* expression in maize mesophyll cells. *Proc. Natl. Acad. Sci. USA*, **98**, 2295-2300.

Figure legends:

Figure 1. *rbcL* transcript accumulation and translation in M and BS cells. A, Upper panel: total RNA (1 µg or the indicated dilution) was isolated from T43 WT total tissue (T), mesophyll protoplasts (M), BS strands (BS), or stressed tissue (TS), and gel blots were hybridized with the probes indicated at right. The ethidium bromide stain is provided as a loading control. Lower panel: relative fold change in *rbcL* and *RBCS* transcript accumulation and purity of cell type extracts was quantified by qRT-PCR from three averaged technical replicates, following normalization to an internal reference gene (*MEP*). Transcripts from the T sample were assigned a reference value of 1. B, polysome analysis was performed from M protoplasts (M) or the mock control (TS), following sedimentation through 15%-55% sucrose gradients. An equal proportion of RNA isolated from each fraction was analyzed by gel blot with the indicated probes. C. Assessment of M cross-contamination by BS, as revealed by *ME* transcript accumulation in M extracts, quantified by qRT-PCR. Samples were analyzed in triplicate, with five and three biological replicates for M and BS extracts, respectively. Error bars represent the standard deviation.

Figure 2. Characterization of *RBCS* RNAi lines. A, construct targeting *RBCS* genes. An *RBCS* inverted repeat, separated by the Rice *waxy* intron, is flanked by the CaMV 35S promoter and the octopine synthase (*ocs*) 3′ UTR. B, *RBCS* mRNA accumulation in a representative ZmsiSS transgenic line. One step semi-quantitative RT-PCR was conducted on total RNA isolated from WT (grown on soil) or the indicated dilutions, and on transformed plantlets grown *in vitro* either expressing the ZmsiSS construct (ZmsiSS) or not (control). Total *RBCS* transcript accumulation was revealed by amplification with the primers hpRBCS cod1 and rev1, which are complementary to both *RBCS1* and *RBCS2* transcripts, for 25 cycles. Amplification of ubiquitin (25 cycles) is presented as a loading control. C, Rubisco LS accumulation in a representative ZmsiSS transgenic plantlet revealed by immunoblot of total proteins extracted from *in vitro*-grown plantlets. Cytochrome *f* was used as a loading control.

Figure 3. Rubisco LS translation is repressed in absence of the SS. Polysome analysis was conducted on an *RBCS* silenced plantlet (ZmsiSS) and an unsilenced control grown *in vitro*. Total leaf extract was sedimented through 15%-55% sucrose gradients. An equal proportion of RNA extracted from each fraction was analyzed by gel blot. Ethidium bromide staining is shown to reflect the similar sedimentation of rRNAs.

Figure 4. Working model for differential Rubisco accumulation in BS versus M cells. Simplified BS (top) and M (bottom) cells are shown with their nuclei (filled circles) and a chloroplast (shaded ovals). In BS, the nuclear *RBCS* genes express Rubisco SS, which is imported into the chloroplast. The chloroplast *rbcL* gene is transcribed, and its mRNA is loaded onto polysomes and translated. Folding of nascent LS may be facilitated by the BSD2 chaperone. Finally, LS and SS assemble to yield the L_8S_8 holoenzyme. In M cells, the *RBCS* genes are not transcribed (cross), and the *rbc*L transcript is not polysome loaded, perhaps leading to its instability. The small amount of translated LS is not assembled, thereby further inhibiting *rbcL* translation due to the CES process.

Figure 5. Ectopic expression of *RBCS* transcripts in M cells. A, schematic of the endogenous *RBCS* genes (top) and the *UbiSSnos* transgenic construct (bottom). Gray and open arrows, *RBCS* and ubiquitin promoters, respectively; horizontal stripes, SS transit peptide (TP); gray rectangles, exons; line, intron; filled and diagonally striped rectangles, *RBCS* and nopaline synthase 3' UTRs, respectively. B, Quantitative RT-PCR determination of the *UbiSSnos* transgene expression, and total *RBCS* transcript abundance from M cells or BS strands of WT

and UbiSS T1 progeny grown in soil. The fold change in expression in this representative qRT-PCR with three technical replicates was normalized to the MEP reference gene and scaled to the sample with the highest expression level for each tested gene, which was defined as 1. *ME* and *MDH* transcript abundance are presented as M to BS ratios to assess cell separation purity. C, total proteins were analyzed by immunoblot after BS/M cell separation. RCA, Rubisco activase; PEPC, Phosphoenolpyruvate carboxylase; ME, Malic enzyme. PEPC is expected to be enriched in M while RCA and ME are enriched in BS. A scan of the Ponceau S-stained membrane (stain) is presented to show loading. D, M extracts from the UbiSS line were fractionated through 15%-55% sucrose gradients, and RNA was extracted to reveal polysome association by Northern blot using an *RBCS* probe. EtBr stain is presented to visualize the rRNA fractionation profile.

Figure 6. Transgenic lines combining ectopic expression of the small and large Rubisco subunits. A, transgenic constructs. Symbols are as described in the legend to Fig. 5; the speckled box represents sequences encoding the Flag epitope. UbiLS_Nnos directs expression of nuclear-encoded LS, whereas UbiSS-LS_N is a single construct containing two transgenes under control of the ubiquitin promoter. B, proteins from WT or UbiSS-LS_N were extracted under native conditions from chloroplast stromal extracts. Proteins (30 µg for the Rubisco immunoblot and 50 µg for the Flag immunoblot) were separated in native 6-15% gradient acrylamide gels and transferred to nitrocellulose, followed by staining with Ponceau-S (left), and probing with anti-LS or anti-Flag antibodies.

Figure 7. Rubisco accumulation and gene expression in UbiSS-LS_N transgenic plants. A, quantitative RT-PCR analysis of *UbiSSnos* and *RbcL_N* transgene expression, and of *RBCS* total accumulation in extracts isolated from M cells of WT T43 and the T1 progeny of UbiSS-LS_N transformants grown in soil. The fold change in expression in this representative qRT-PCR with three technical replicates was normalized to the MEP reference gene and scaled to the sample with the highest expression level for each tested gene, which was defined as 1. *ME* and *MDH* transcript abundance are presented as M to BS ratios to assess cell separation purity. B, immunoblot analysis of M or BS total proteins, using the antibodies shown at right. The lower panel is a Ponceau-S stained membrane, for which the image has been vertically compressed. C, polysome analysis of a M extract from UbiSS-LS_N F1 progeny, by Northern analysis with probes indicated at right.

Figure 8. Immunolocalization of Flag-tagged and total LS. A, differentiated tissue (tip of the third leaf) from the genotypes indicated at left were analyzed by thin sectioning and immunodetection of the Flag epitope (red false color) and Rubisco (green false color). Fluorescence signals were overlaid on differential interference contrast images (DIC) to show their positions relative to leaf structures. For Flag immunodetection, chlorophyll autofluorescence was minimal, as it is not strongly excited at 594 nm. For LS immunolocalization, LS was imaged from 498-517 nm, and chlorophyll autofluorescence from 659-740 nm (red false color). B, Immunolocalization of LS_N in etiolated plants using anti-Flag antibody. The confocal images are an overlay of the 616-634 nm fluorescence signal with brightfield images.

Figure 9. Overall Rubisco accumulation in transgenic lines. A, immunoblot analysis of total proteins from the genotypes indicated at the top, with cytochrome *f* as a loading control. B, quantification of Rubisco LS, relative to cytochrome *f*, as measured by at least three biological replicates, with standard errors shown. C, Immunoblot analysis was performed on total proteins from the genotypes indicated at left, or on purchased protein standards for LS or a Flag epitope-containing protein. Protein standard amounts are shown in pmol, and total protein amounts in

µL. Amounts from the two transgenic lines cannot be compared directly because the total protein samples are of different concentrations.

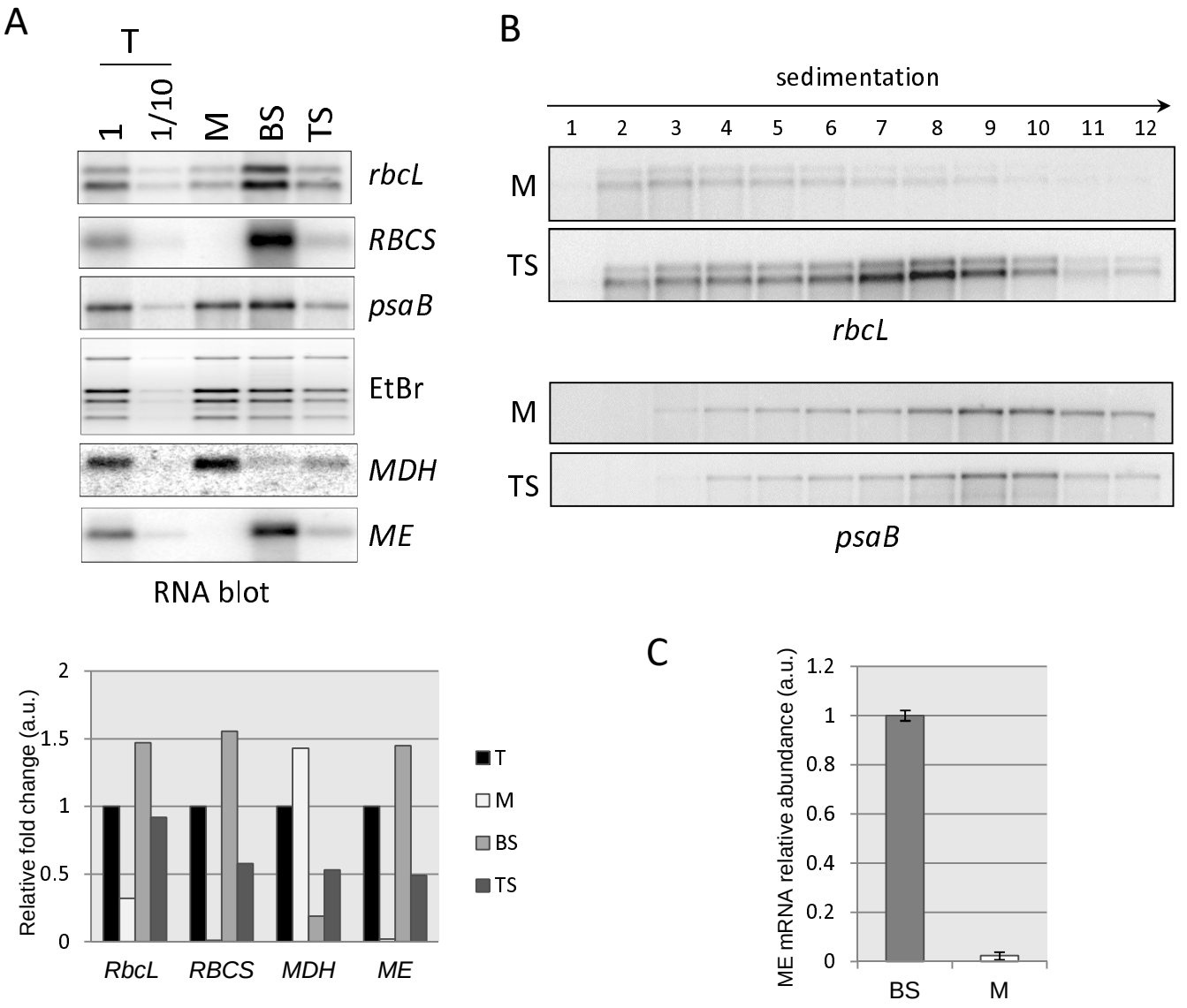

Figure 1. *rbcL* transcript accumulation and translation in M versus BS cells. A, Upper panel: total RNA (1 µg or the indicated dilution) was isolated from T43 WT total tissue (T), mesophyll protoplasts (M), BS strands (BS), or stressed tissue (TS), and gel blots were hybridized with the probes indicated at right. The ethidium bromide stain is provided as a loading control. Lower panel: relative fold-change in the *rbcL* and *RBCS* transcript accumulation and purity of the cell type extracts of a representative experiment with technical replicates (n=3) was quantified by qRT-PCR, after normalization to an internal reference gene (MEP). Transcripts from total extracted were used as calibrator, and assigned a value of 1. B, polysome analysis was performed from M protoplasts (M) or the mock control (TS), following fractionation through 15%-55% sucrose gradients. An equal proportion of RNA isolated from each fraction was analyzed by gel blot with the indicated probes. C. Assessment of M cross-contamination by BS, as revealed by *ME* transcript accumulation in M extracts, quantified by qRT-PCR analysis (samples done in triplicates, with respectively 5 and 3 biological replicates for M and BS extracts. Error bars represent the standard deviation.

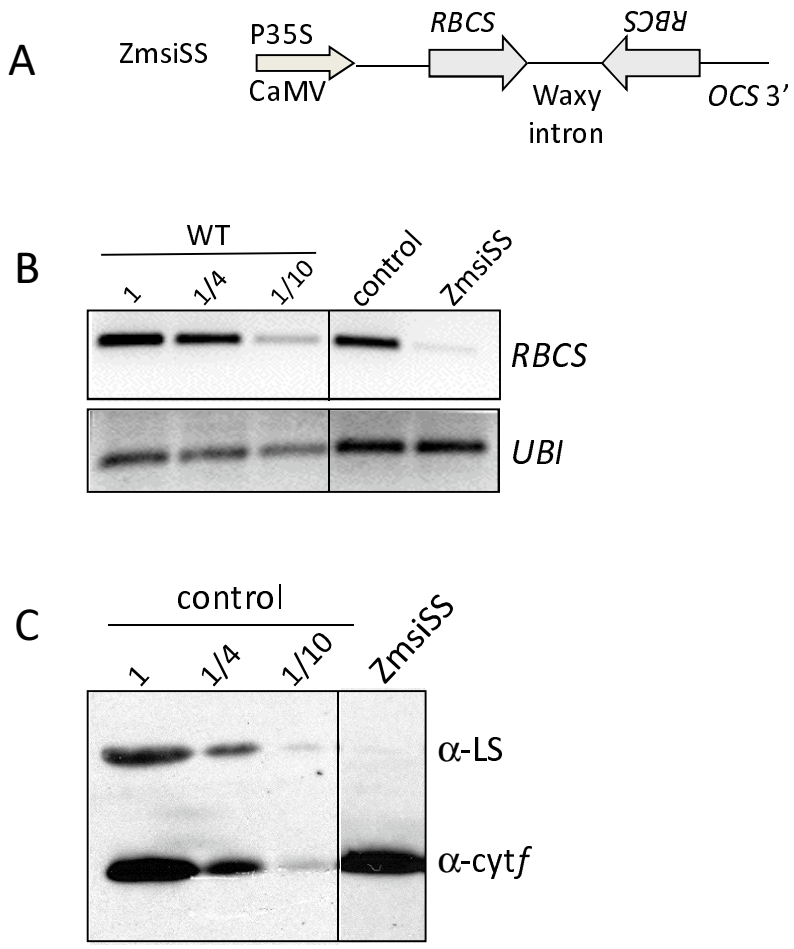

Figure 2. Characterization of *RBCS* RNAi lines. A, construct targeting *RBCS* genes. An *RBCS* inverted repeat, separated by the Rice *waxy* intron, is flanked by the CaMV 35S promoter and the octopine synthase (*ocs*) 3′ UTR. B, *RBCS* mRNA accumulation in a representative ZmsiSS transgenic line. One step semi-quantitative RT-PCR was conducted on total RNA isolated from WT (grown on soil) or the indicated dilutions, and on transformed plantlets grown *in vitro* either expressing the ZmsiSS construct (ZmsiSS) or not (control). Total *RBCS* transcript accumulation was revealed by amplification with the primers hpRBCS cod1 and rev1, which are common to both *RBCS1* and *RBCS2* transcripts, for 25 cycles. Amplification of ubiquitin (25 cycles) is presented as a loading control. C, Rubisco LS accumulation in a representative ZmsiSS transgenic plantlet revealed by immunoblot of total proteins extracted from *in vitro*-grown plantlets. Cytochrome *f* was used as a loading control.

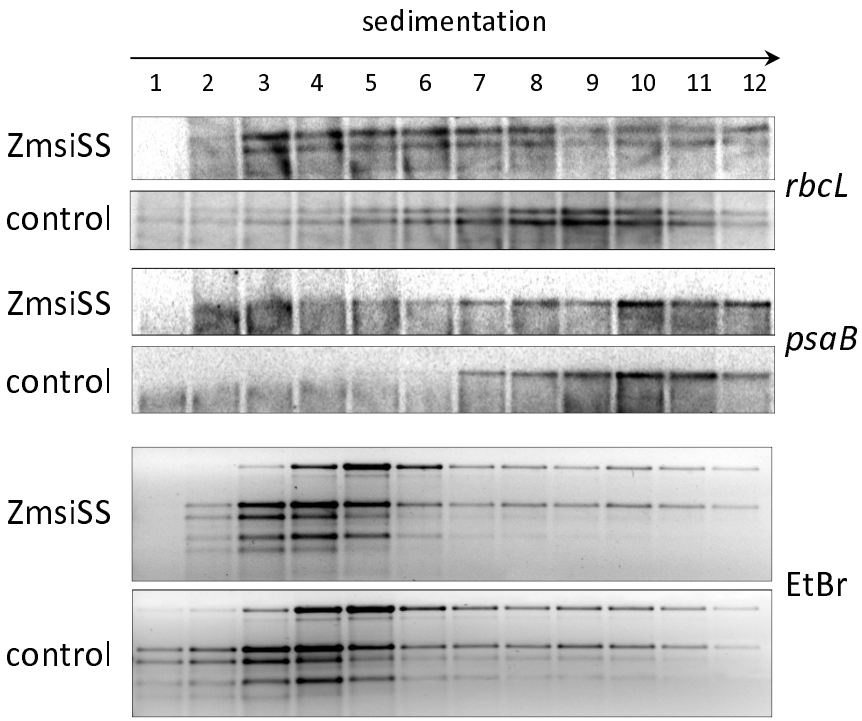

Figure 3. Rubisco LS translation is repressed in absence of the SS. Polysome analysis was conducted on an *RBCS* silenced plantlet (ZmsiSS) and an unsilenced control grown *in vitro*. Total leaf extract was fractionated through 15%-55% sucrose gradients. An equal proportion of RNA extracted from each fraction was analyzed by gel blot. Ethidium bromide staining is shown to reflect the similar sedimentation of rRNAs.

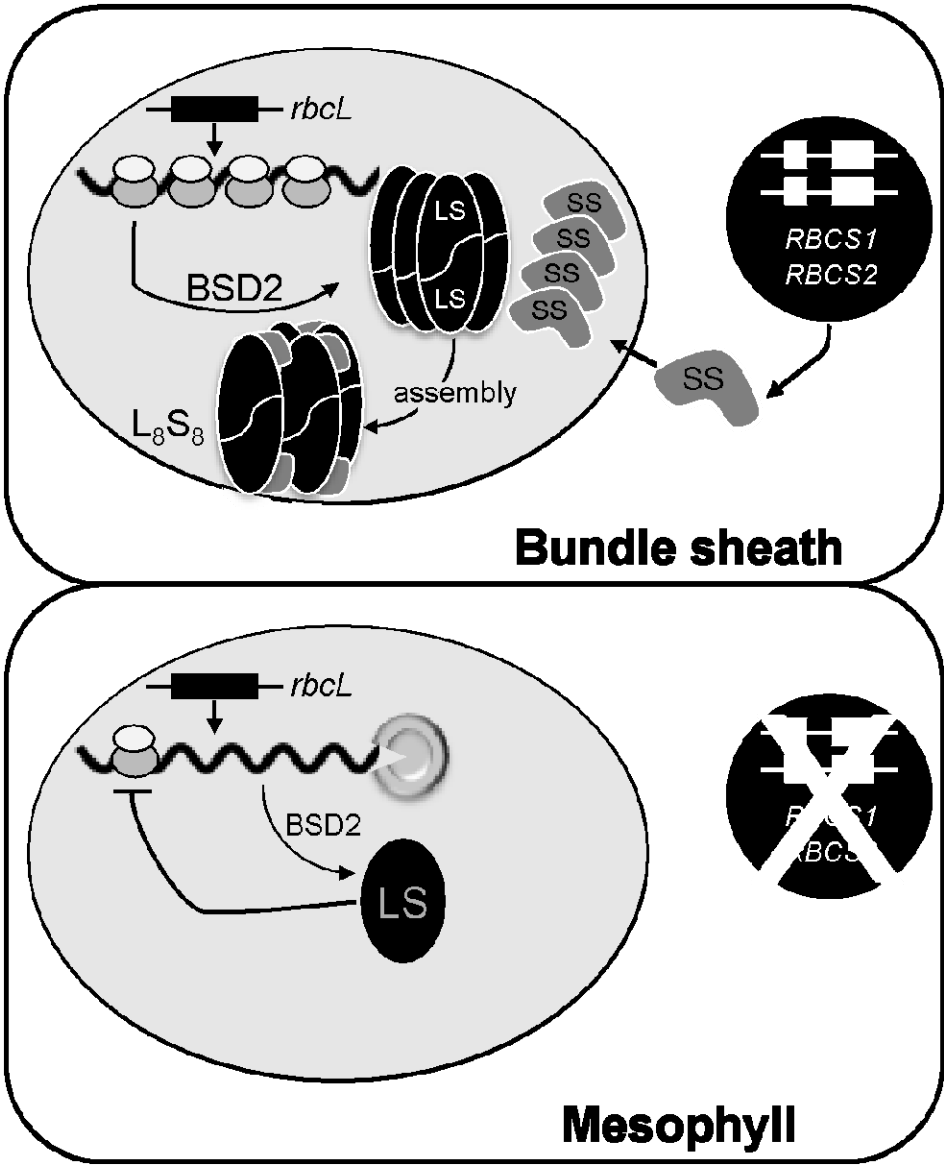

Figure 4 . Working model for differential Rubisco accumulation in BS versus M cells. Simplified BS (top) and M (bottom) cells are shown with their nuclei (filled circles) and a chloroplast (shaded ovals). In BS, the nuclear *RBCS* genes express Rubisco SS, which is imported into the chloroplast. The chloroplast *rbcL* gene is transcribed, and its mRNA is loaded onto polysomes and translated. Folding of nascent LS may be facilitated by the BSD2 chaperone. Finally, LS and SS assemble to yield the L8S8 holoenzyme. In M cells, the *RBCS* genes are not transcribed (cross), and the *rbc*L transcript is not polysome loaded, perhaps leading to its instability. The small amount of translated LS is not assembled, thereby further inhibiting *rbcL* translation due to the CES process.

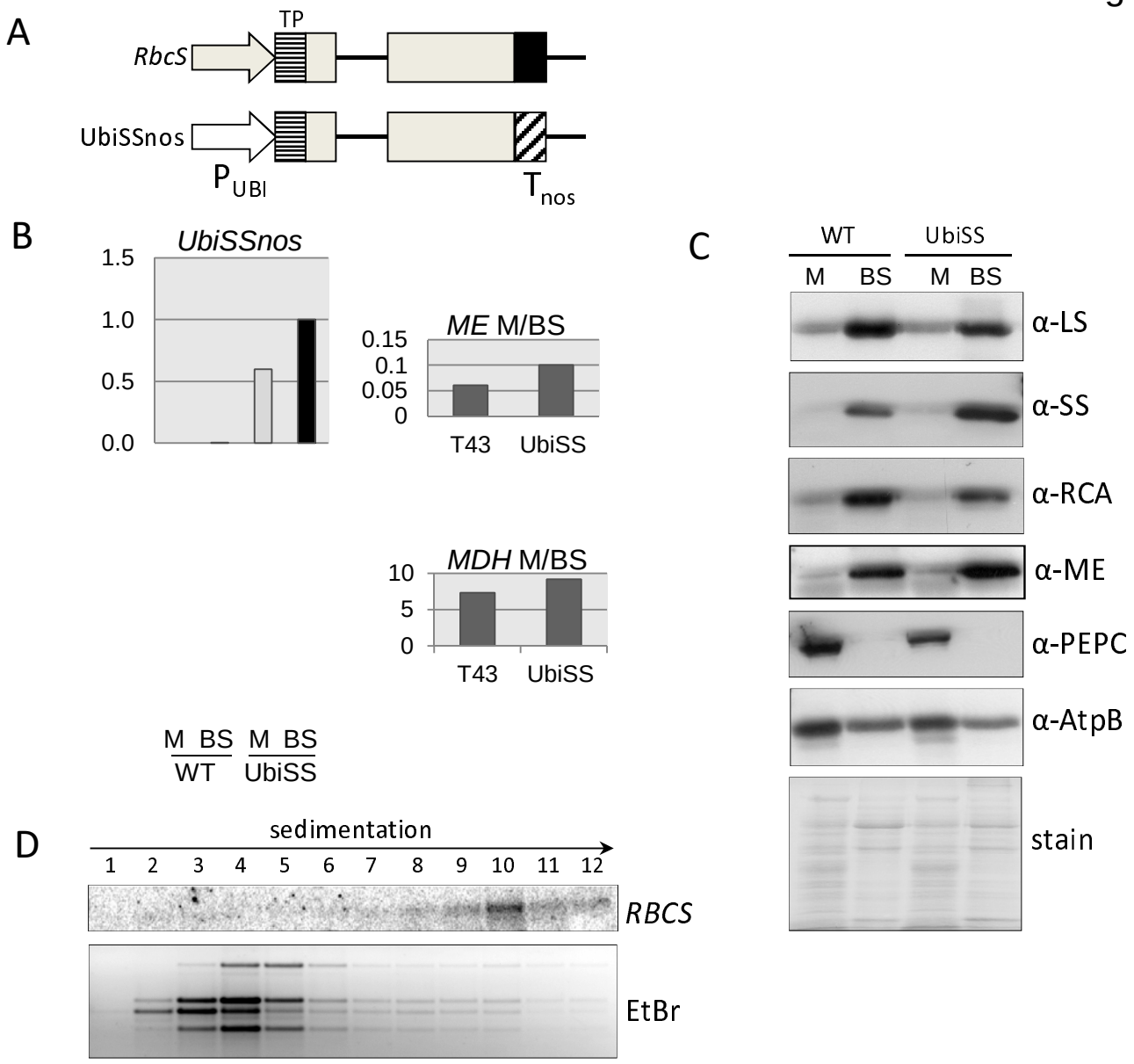

Figure 5. Ectopic expression of *RBCS* transcripts in M cells. A, schematic of the endogenous *RBCS* genes (top) and the *UbiSSnos* transgenic construct (bottom). Gray and open arrows, *RBCS* and ubiquitin promoters, respectively; horizontal stripes, SS transit peptide (TP); gray rectangles, exons; line, intron; filled and diagonally striped rectangles, *RBCS* and nopaline synthase 3' UTRs, respectively. B, Quantitative RT-PCR determination of the *UbiSSnos* transgene expression, and total *RBCS* transcript abundance from M cells or BS strands of WT and UbiSS T1 progeny grown in soil. The fold change in expression in this representative qRT-PCR with three technical replicates was normalized to the MEP reference gene and scaled to the sample with the highest expression level for each tested gene, which was defined as 1. *ME* and *MDH* transcript abundance are presented as M to BS ratios to assess cell separation purity. C, total proteins were analyzed by immunoblot after BS/M cell separation. RCA, Rubisco activase; PEPC, Phosphoenolpyruvate carboxylase; ME, Malic enzyme. PEPC is expected to be enriched in M while RCA and ME are enriched in BS. A scan of the Ponceau S-stained membrane (stain) is presented to show loading. D, M extracts from the UbiSS line were fractionated through 15%-55% sucrose gradients, and RNA was extracted to reveal polysome association by Northern blot using an *RBCS* probe. EtBr stain is presented to visualize the rRNA fractionation profile.

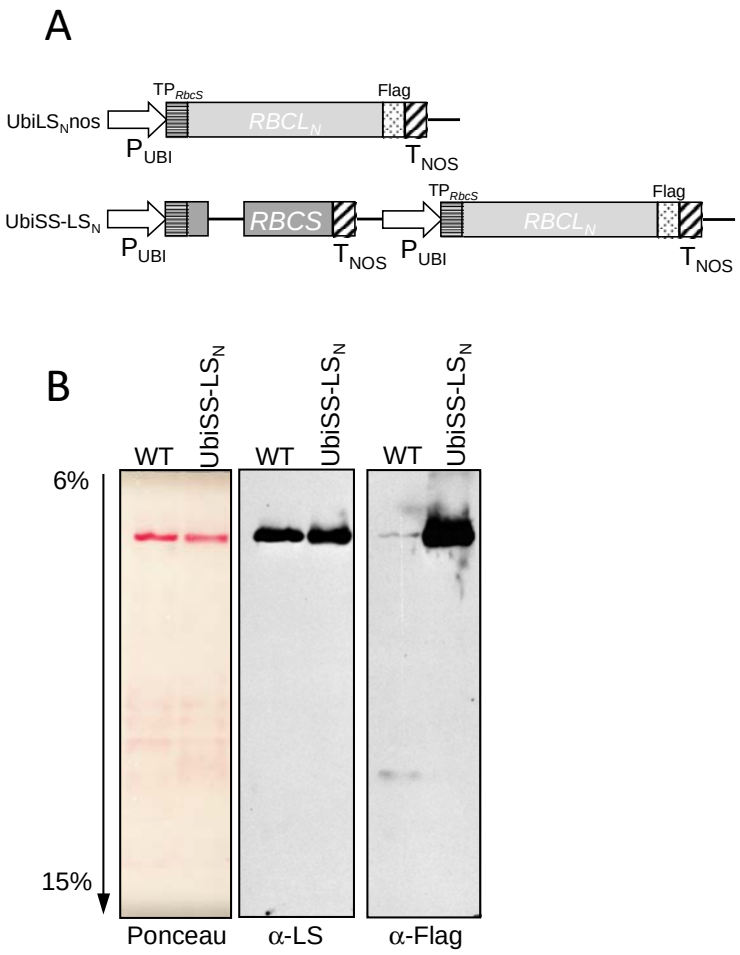

Figure 6. Transgenic lines combining ectopic expression of the small and large Rubisco subunits. A, transgenic constructs. Symbols are as described in the legend to Fig. 5; the speckled box represents sequences encoding the Flag epitope. UbiLS$_N$nos directs expression of nuclear-encoded LS, whereas UbiSS-LS$_N$ is a single construct containing two transgenes under control of the ubiquitin promoter. B, proteins from WT or UbiSS-LS$_N$ were extracted under native conditions from chloroplast stromal extracts. Proteins (30 µg for the Rubisco immunoblot and 50 µg for the Flag immunoblot) were separated in native 6-15% gradient acrylamide gels and transferred to nitrocellulose, followed by staining with Ponceau-S (left), and probing with anti-LS or anti-Flag antibodies.

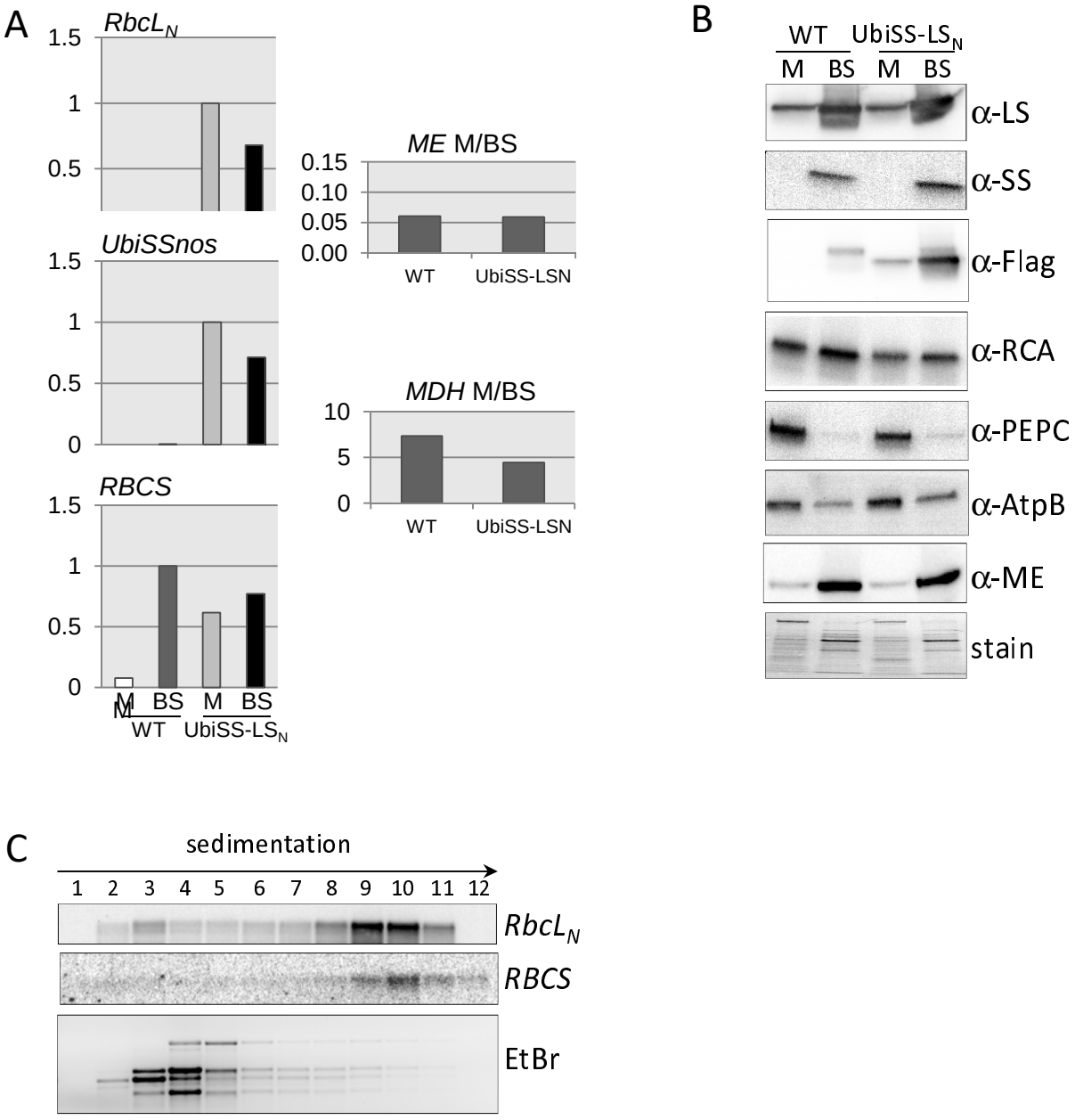

Figure 7. Rubisco accumulation and gene expression in UbiSS-LS$_N$ transgenic plants. A, quantitative RT-PCR analysis of *UbiSSnos* and *RbcL$_N$* transgene expression, and of *RBCS* total accumulation in extracts isolated from M cells of WT T43 and the T1 progeny of UbiSS-LS$_N$ transformants grown in soil. The fold change in expression in this representative qRT-PCR with three technical replicates was normalized to the *MEP* reference gene, and scaled to the sample with the highest expression level for each tested gene, which was defined as 1. *ME* and *MDH* transcript abundance are presented as M to BS ratios to assess cell separation purity. B, immunoblot analysis of M or BS total proteins, using the antibodies shown at right. The lower panel is a Ponceau-S stained membrane, for which the image has been vertically compressed. C, polysome analysis of a M extract from UbiSS-LS$_N$ F1 progeny, by Northern analysis with probes indicated at right.

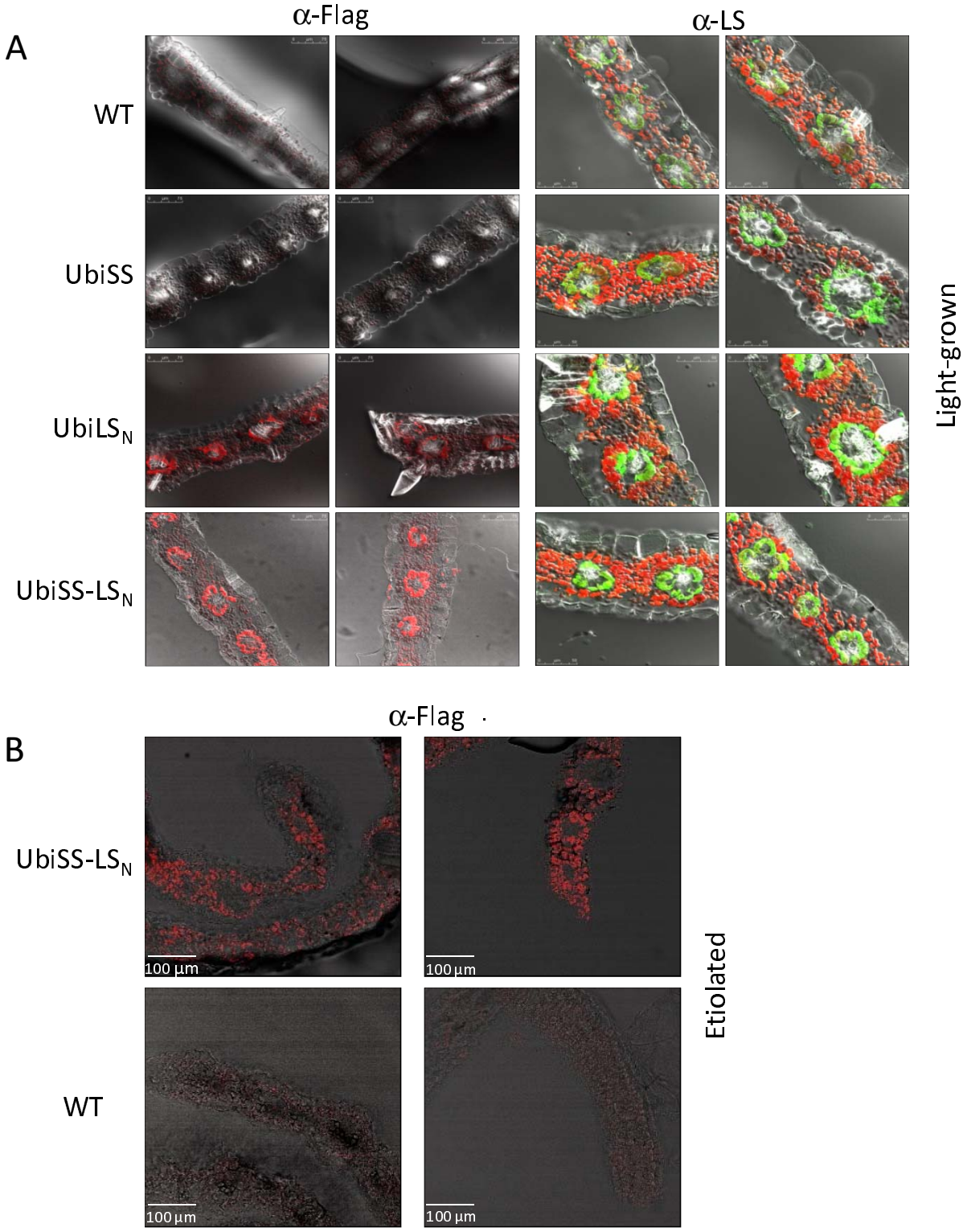

Figure 8. Immunolocalization of Flag-tagged and total LS. A, differentiated tissue (tip of the third leaf) from the genotypes indicated at left were analyzed by thin sectioning and immunodetection of the Flag epitope (red false color) and Rubisco (green false color). Fluorescence signals were overlaid on differential interference contrast images (DIC) to show their positions relative to leaf structures. For Flag immunodetection, chlorophyll autofluorescence was minimal, as it is not strongly excited at 594 nm. For LS immunolocalization, LS was imaged from 498-517 nm, and chlorophyll autofluorescence from 659-740 nm (red false color). B, Immunolocalization of LS_N in etiolated plants using anti-Flag antibody. The confocal images are an overlay of the 616-634 nm fluorescence signal with brightfield images.

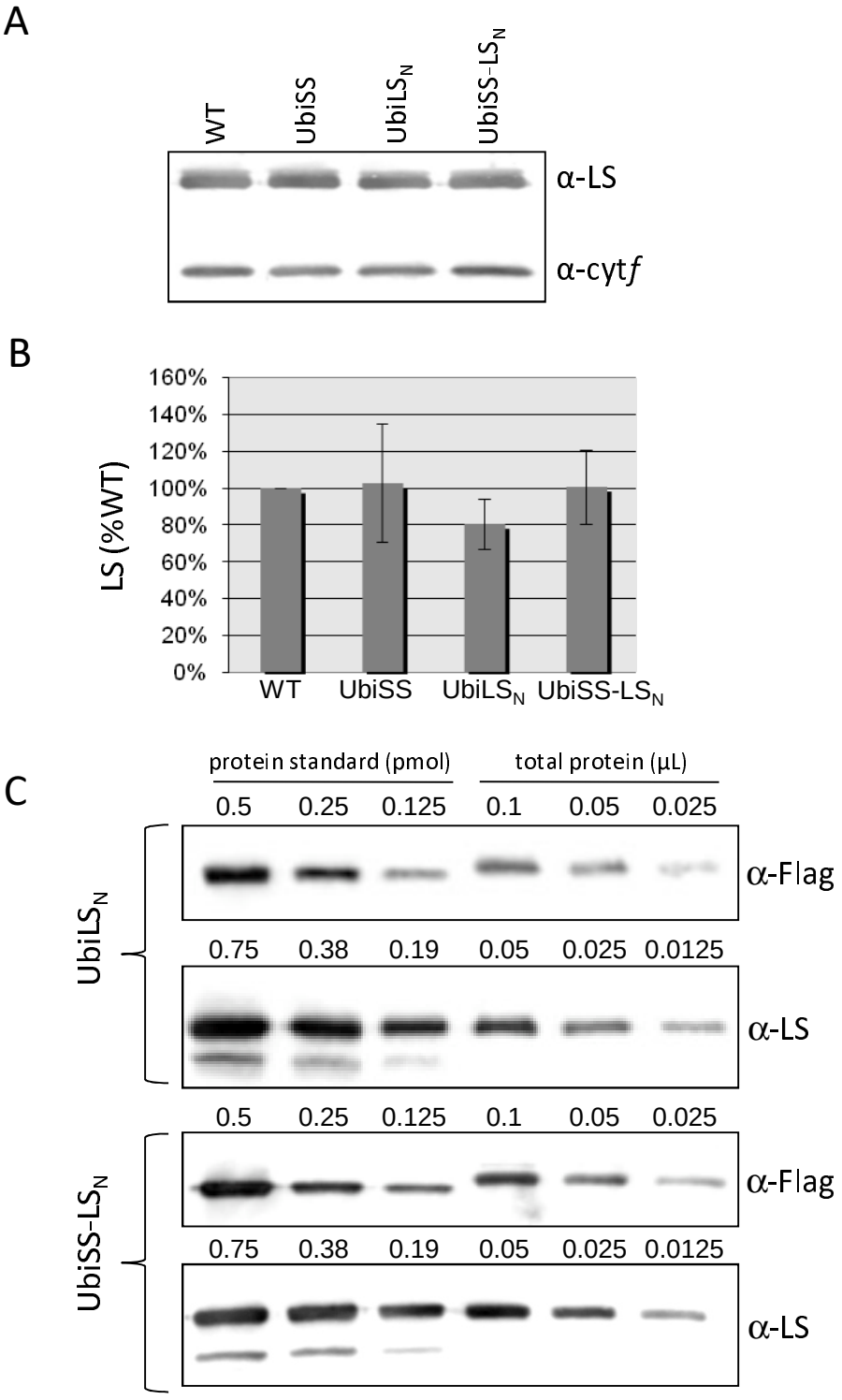

Figure 9. Overall Rubisco accumulation in transgenic lines. A, immunoblot analysis of total proteins from the genotypes indicated at the top, with cytochrome *f* as a loading control. B, quantification of Rubisco LS, relative to cytochrome *f*, as measured by at least three biological replicates, with standard errors shown. C, Immunoblot analysis was performed on total proteins from the genotypes indicated at left, or on purchased protein standards for LS or a Flag epitope-containing protein. Protein standard amounts are shown in pmol, and total protein amounts in µL. Amounts from the two transgenic lines cannot be compared directly because the total protein samples are of different concentrations.

TABLE S1. Primer sequences (restriction sites in *italics*)	
Primer Name	**Sequence**
hpRBCS cod1	AAACTAGTGGCGCGCCGGCCTACGGCAACAAGAAGTT
hpRBCS rev1	AAGCGATCGCCCTAGGGGCTTGTAGGCGATGAAGCTG
ZM-rbcL 5'	GCAGTAGCTGCGGAATCTTCTACT
ZM-rbcL 3'	GGTGAATGTGAAGAAGTAGGCCGT
RBCS1 AUG HindIII	GT*AAGCTT*ATGGCGCCCACCGTGATGA
RBCS1 revCla	GG*ATCGATC*TAGTCGCTGCCCGGGGGCT
Nos-ClaI	TT*ATCGAT*GCAGATCGTTCAAACATTTGGC
Nos-ApaI	TT*GGGCCC*GATCTAGTAACATAGATGACAC
Zm-MDH5’	GAATGCCAAAATTGATGGAAGACC
Zm-MDH3’	GCATCATAGTCAATTCGTGTGG
Zm-ME5’	GATCGGGACATCTGGAGTGG
Zm-ME3’	CAGGTACAATGCCTCTCCAGC
ZmUbi2.1 fw	CTACAACATTCAGAAGGAGAGCAC
ZmUbi2.2 rev	TCTGCAAGGGTACGGCCATCC
Zm-psaB 5’	CGCTGTGGAAGCCTTTACTC
Zm-psaB 3’	CCTTTATGCCCACGTCCTAA
Nos RT rev2	ACATGCTTAACGTAATTCAAC
NuLS fw2	CCGCACGGCATCCAGGTGGA
NuLS rev2	CGGTGCCGGAGTGGATGTGA
RBCS cod2	GGAAGGATCCGGTGCATGCAG
RBCS1 rev1	GAACCATGGCCGGGGAAAAGA
ZmRBCSTP-NuRbcL.F	ATGGATCCGGTGCATGTCCCCGCAGACCGAGACC
ZmNuRbcL flag tag.R	AGGATCGATTCATTTGTCGTCGTCGTCTTTGTAGTCGAT GGTGTCCATCGCCTT
HCnospBS delta Bam QC1	CAGCCCGGGGCATCCACTAGTTCTA
HCnospBS delta Bam QC2	TAGAACTAGTGGATGCCCCGGGCTG
ZmMEqF1	TGGCAGAGCAGACGTATTTG
ZmME qR1	TGAAGGGAGCCTTTACGAGA
ZmMDH qF1	TCACCTGCTGTTCAAACTCG
ZmMDH qR1	GGATACAGCGAGTCCTCCAG
ZmMEP qF1	TGTACTCGGCAATGCTCTTG
ZmMEP qR1	TTTGATGCTCCAGGCTTACC
ZmqLS-1F	AAGGGGAACGCGAAATAACT
ZmqLS-123R	AGGCTTCTAAAGCCACACGA
ZmRbcS qR4	TGAACTCGAGGCAGGGTATC
ZmNurbcL qF3	ACGACGAGAACGTGAACTCC
ZmNurbcL qR3	GTTGAGGTAGTGGCCCTTGA
ZmUbiSSnos qF1	CCACCCAGGTGTACAAGGAG
ZmUbiSSnos qR1	ATTGCCAAATGTTTGAACGA